Paper AAS 03-113

CONTROL STRATEGIES FOR FORMATION FLIGHT IN THE VICINITY OF THE LIBRATION POINTS

K.C. Howell and B.G. Marchand
School of Aeronautics and Astronautics
Purdue University
West Lafayette, Indiana 47907-1282

13th AAS/AIAA Space Flight Mechanics Meeting

Ponce, Puerto Rico **9-13 February 2003**

AAS Publications Office, P.O. Box 28130, San Diego, CA 92198

AAS 03-113

CONTROL STRATEGIES FOR FORMATION FLIGHT IN THE VICINITY OF THE LIBRATION POINTS

K.C. Howell,[1] and B.G. Marchand[2]

The concept of formation flight of multiple spacecraft offers many promising possibilities both for space exploration and the associated technology development. Recent studies have focused primarily on formation flight for Earth-orbiting clusters. However, space based observatory and interferometry missions, such as Starlight (ST3) [1-2], Terrestrial Planet Finder (TPF) [3-4], Planet Imager [5], and Life Finder [6], have sparked new interest in formation flight in multi-body regimes, particularly in the vicinity of the Sun-Earth-Moon (SEM) libration points. The goal of this study is to develop some basic understanding about the natural formation dynamics in the CR3BP. Then, the baseline propulsive requirement, for a variety of formation configurations, is determined. The effectiveness of existing control techniques in maintaining the prescribed formations is also investigated. A de-centralized control strategy is presented based on optimal and nonlinear control methods. Both techniques have been successfully implemented and tested on a two-S/C formation evolving along periodic and quasi-periodic orbits near the SEM L_1 and L_2 libration points.

INTRODUCTION

For this study, "formation flight" is defined as a number of satellites that maintain a constant relative distance, and perhaps orientation, over long periods of time. In general, this type of dynamical configuration is not likely to exist as natural motion in either the two-body problem (2BP) or a multi-body regime. Much of the research to date refers to the control of constellations, clusters, and formations for Earth-orbiting missions [7-23] where the influence of other gravitational perturbations can be safely ignored. However, recent interest in formation flight near the Sun-Earth libration points requires an assessment of the effectiveness of the more commonly implemented control techniques. The nature of the dynamical force model in this region of space does not allow an analytical solution for the reference path of a spacecraft. Although some approximations are available, any analysis involving formation flight in multi-body systems is still strongly dependent on numerical methods.

In the two-body regime, optimal control techniques are the most commonly encountered in the available literature on formation flight [7-16]. Many of these references reasonably assume that the formations are relatively small. Hence, the reference motion is modeled completely in terms of the linearized dynamics, as described by the Clohessy-Wiltshire equations in the 2BP. Thus, the controller is applied to the linear system and its effectiveness in the nonlinear model is not explicitly demonstrated. Impulsive control

[1] Professor, School of Aeronautics and Astronautics, Purdue University, West Lafayette, IN 47907
[2] Graduate Student, School of Aeronautics and Astronautics, Purdue University, West Lafayette, IN 47907

schemes have also been implemented but are only applicable to formations that do not require constant tracking of a reference solution [17-19]. This approach is usually based on a Keplerian formulation of the two-body dynamics. Nonlinear methods, such as Lyapunov based control [20-21] combined with adaptive control methods [22-23] have also been successfully implemented for small formations in the two-body regime. Among these researchers, only de Queiroz et al. [22-23] developed their control strategies based solely on the full nonlinear equations of motion.

Control strategies for formation flight in multi-body systems are much less common and the increased degree of complexity associated with the dynamical model usually extends to the control as well. Gurfil and Kasdin [24] consider formation-keeping strategies based on optimal control (LQR) in the Circular Restricted Three-Body Problem (CR3BP). The nominal formation employed in their study corresponds to one that is fixed in distance and orientation relative to the Sun-Earth rotating frame. The particular reference trajectory that is described in reference [24], however, was apparently based on a set of initial conditions corresponding to a 200 km altitude circular Earth orbit, subject to an applied impulsive out-of-plane maneuver of 4.9 km/sec. For the dynamical model presented in their study, this set of initial conditions does not appear to be consistent with the trajectory presented in the visuals (however, the precise configuration of the initial conditions is unknown). Furthermore, even for an accurate model, any similar set of initial conditions will not yield the type of motion that is characteristic near the Sun-Earth libration points, that is, periodic and quasi-periodic orbits or the associated stable and unstable manifolds. Hence, the effectiveness of this approach is not actually demonstrated for this highly sensitive region of space nor was it ever a goal of their analysis.

Another study, by Scheeres and Vinh [25], considers motion relative to an unstable orbit in Hill's problem. In particular, the vehicle dynamics are modeled as a perturbation relative to an unstable nominal halo orbit near the Sun-Earth L_2 point. The goal is a controller that maintains bounded motion around the nominal path rather than the tracking of some specific motion relative to the halo orbit. The control problem is simplified by reducing the time-varying nature of the linear system into a series of discrete segments, each assumed to be accurately described by locally time invariant dynamics. Hence, the system matrix associated with each segment is defined as constant. This approach is somewhat similar to gain scheduling. The controller is designed using information about the "local" stable and unstable eigenvectors of the system matrix associated with each segment along the path. As noted by the authors, this type of control scheme is most appropriate when the relative dynamics of each spacecraft in the formation are not expected to track some prescribed path or precise distance/orientation at all times.

Howell and Barden [26-28] have also investigated formation flying near the vicinity of the libration points in the CR3BP. Initially, their focus is the determination of the natural behavior on the center manifold near the libration points and the first stage of their study captured a naturally occurring six-satellite formation near the libration points [26]. Further analysis considered strategies to maintain a periodic, planar formation of the six vehicles in an orbit about the Sun-Earth L_1 point [27-28]. The deviation of each spacecraft is controlled impulsively relative to the plane of the initial formation, one that is specified to be contained within the center manifold. The natural flow in the center subspace is such that the relative distances between each spacecraft remain essentially bounded and the relative configuration of the formation is time independent.

The present study, then, represents an effort to survey existing control strategies and assess their effectiveness in the multi-body problem, in particular, for libration point missions in the Sun-Earth-Moon (SEM) system. In contrast to some earlier efforts, relative distance and orientation are constrained. Optimal control techniques for time-varying systems are successfully applied. Nonlinear control methods are also

considered and the performance between both approaches is contrasted. The relative dynamics of the formation are modeled in terms of cartesian coordinates, relative to the chief spacecraft, and a de-centralized control approach is employed. Hence, the control of each spacecraft is independent of the other and the goal is to successfully track some prescribed nominal distance and/or orientation at all times. As an example, formations that are fixed relative to the rotating or inertial frames are considered as well as the less constrained problem of distance tracking. Quasi-periodic nominal motion on a torus surrounding a halo orbit is also investigated and successfully controlled via optimal and nonlinear control techniques.

BACKGROUND

Previous Work

Of the control strategies previously applied in the two-body regime, LQR and feedback linearization, a basic nonlinear control approach, are considered in the present study of formation flight in the CR3BP. Notably, Irvin and Jacques [13] consider a combination of LQR with feedback linearization. In this section, some details of their approach are discussed to contrast the effectiveness of each control scheme as applied to formation flight in the two- and three-body models. Although Gurfil and Kasdin [24] consider LQR control in a CR3B model, their analysis does not encompass the type of reference motion that is the focus of the formation flight analysis here. In particular, formations in this work evolve in the vicinity of the libration points in the circular restricted three-body problem (CR3BP). Scheeres and Vinh [25], Hamilton [29], and Folta et al. [30] do consider control strategies near the libration points. Thus, these three methodologies are briefly discussed to establish the differences between these previous approaches and the control strategies implemented in this study.

LQR and Feedback Linearization in the 2BP

Irvin and Jacques [13] investigate satellite formation control in the two-body problem. In particular, a two-spacecraft formation is controlled such that the chief spacecraft follows a 10,000 km circular orbit around the Earth and the deputy is commanded to maintain some nominal separation at all times. The formations considered in their study range from one to forty kilometers in separation for some prescribed formation orientation. Three control methods are considered: a standard LQR controller based on the linearized Clohessy-Wiltshire equations, a nonlinear controller that uses both Input Feedback Linearization (IFL) combined with LQR to ensure accurate tracking, and a standard discrete station-keeping approach. Feedback linearization is applied to the full nonlinear equations to cancel the nonlinear gravity terms. The residual linear dynamics are controlled via a standard LQR approach. Since the new linear system matrix is constant, the algebraic Riccatti equation is solved to compute the gain matrix. Their results reveal that both LQR and nonlinear control yield essentially identical results for the smaller formations (~ 1 km). However, the nonlinear control techniques are most effective for the larger formations (~40 km). In their study, Irvin and Jacques note that sometimes "*the nonlinear controller might produce inferior results,*" particularly for the smaller one kilometer formations. However, this may be due to the combination of the LQR with the IFL. If the controller is completely nonlinear, the results may be different. It is true, however, that sometimes feedback linearization techniques may require prohibitive formationkeeping costs. This issue must be addressed on a case-by-case basis since it is extremely model dependent. Since feedback linearization techniques essentially change the dynamics of the problem by eliminating the nonlinearities, the controller is required to cancel gravity and expend more effort to force the response to track the desired solution. This very fact suggests that feedback linearization may be well-suited for application to the 3BP near the libration points. Since the net gravitational forces in this region of space are much weaker than in Earth orbit, feedback linearization can produce very reasonable results. In the present study, both input and

output feedback linearization are considered and successfully implemented in the CR3BP. In all the cases presented here, the formation keeping cost is similar to or better than that determined from LQR techniques over a wide operating range.

Formation Control Strategies in the CR3BP

Scheeres and Vinh [25] consider "formation flight" within the context of Hill's problem. Hill's model is usually appealing because it reduces the nonlinear system to a less complex form. However, the assumptions associated with this model do have notable consequences in terms of the solution space. In particular, the number of equilibrium points is reduced from five to two, essentially equivalent to L_1 and L_2. A further difference, in comparison to the full CR3B model, is that near these equilibrium points, the "halo" families themselves are symmetric across the *yz*-plane. This is not the case in the CR3BP where, near the smaller primary, the hodographs representing the L_1 and L_2 halo families approach an asymptote from opposite sides and the amplitudes progress in different directions. More specifically, the out-of-plane amplitude of members along the L_1 family tends to infinity as it approaches the asymptote from one side while the L_2 family collapses towards the primary along the opposite side of the asymptote. These observations are significant for studies, such as the current investigation, that include halo orbits along an entire family.

In their study, Scheeres and Vinh define a nominal as, roughly, a 300,000 km out-of-plane amplitude "halo" orbit near the L_2 libration point. A set of variational equations of the form $\delta\dot{\bar{x}}(t) = A(t)\delta\bar{x}(t)$, derived relative to this nominal, governs the motion of the vehicle. The linearized dynamics are further simplified by assuming that, over a sufficiently small time interval δt, the matrix $A(t_i)$ remains roughly constant. Hence, the state transition matrix can be written as a function of the matrix exponential $\exp(A(t_i))$. The matrix exponential is then approximated via a truncated Taylor series that includes only the linear terms in δt. Of course, from general linear systems theory, if the state $\bar{x}(t_i)$ on the periodic orbit were instead an equilibrium point, this approximation would imply that the local stability of the equilibrium point, $\bar{x}(t_i)$, is dependent on the eigenstructure of the matrix $A(t_i)$, which is assumed to remain constant over the interval δt. The controller is then modeled based on an approximation of the local pseudo-linearized dynamics at each state along the path. In essence, the vehicle dynamics are modeled as a perturbation relative to the nominal "halo" orbit. Hence, the apparent goal is to construct a controller that achieves "local", not global, marginal stability such that the spacecraft remains in the immediate vicinity of the halo orbit. The proposed controller is formulated from knowledge of the stable and unstable eigenvectors of the local matrix $A(t_i)$. By treating $\bar{x}(t_i)$ as a local "equilibrium" point, such that $A(t_i)$ is constant, these eigenvectors represent the stable and unstable directions associated with $\bar{x}(t_i)$. The controller gain matrix is then formed by the addition of two matrices that project the initial perturbation onto the "local" stable and unstable subspaces with the objective that the perturbation neither grows nor decays. For a sufficiently high gain, the controller proves to be effective in achieving "bounded" motion over the period of time considered in the study. An added advantage of this approach is that it is relatively simple to implement. However, since the system is, in fact, time-varying, there is no guarantee that the controller will be successful for all time or for all reasonable perturbations. The present work differs from Scheeres and Vinh [25] in some fundamental ways. In this analysis, relative distance is fixed and total cost per revolution defines a successful control. With different goals, Scheeres and Vinh achieve acceleration levels that are very low, but the total propulsive cost over one revolution is relatively high. For example, one sample case in the analysis here corresponds to a formation separation of 5000 km. Using the approach proposed by Scheeres and Vinh results in a trajectory that is bounded between 18 km and 5000 km relative to the original halo orbit. The acceleration level never exceeds 3×10^{-4} m/sec^2. However, the total cost required to stabilize the orbit, over one orbital period of the original halo (6 months), is 1.68 km/sec. The

current study also considers responses to velocity injection errors, an analysis not presented by Scheeres and Vinh [25]. A point of note, in general and non-exclusive to formation flight applications, if bounded tracking of the original halo orbit is a requirement, it has been numerically determined that this controller does not to respond well to large velocity injection errors, e.g., on the order of 1 km/sec. In the present study, both optimal and nonlinear control strategies usually respond to this type of error but, not surprisingly, the correction cost is on the same order of magnitude as the velocity injection error.

Hamilton [29] studies the problem of multi-spacecraft formation flight within the context of the CR3BP. In particular, the study considers LQG control as applied to the station-keeping problem, as well as formation slewing and reorientation. Hamilton uses an approach similar to that of Scheeres and Vinh by assuming the $A(t_i)$ matrix to remain roughly constant over a specified time interval and computing the "optimal" controller for that interval in the presence of process noise. By assuming an "infinite" horizon, determination of the controller gain matrix is reduced to computing the solution to the discrete algebraic Riccatti equation at each time step. Although the initial development is based on a linear approximation of the Lissajous orbit, the actual implementation of the controller is performed in the full ephemeris model. To do this, Hamilton relies on software developed at Purdue University [31] to compute a true Lissajous trajectory in the full nonlinear ephemeris system. In this model, no assumptions are made about the motion of the primaries, hence the numerical integration uses actual planetary ephemeris to determine the position of the Earth at any given time. Furthermore, Hamilton also includes lunar perturbations in the model. The nominal trajectory, determined via a two-level differential corrections process applied to an initial approximation, is then stored for later use to compute the LQG controller gain matrix. Naturally, the assumptions associated with the implementation of this controller do not satisfy all the constraints derived from optimal control theory for time varying systems. Hence, there is no guarantee that the resulting controller is optimal or that it works over a wide operating range, though it appears to be quite effective.

Folta, Carpenter, and Wagner [30] use an approach slightly similar to Hamilton [29]. In their study, a decentralized control approach is developed using LQR techniques combined with disturbance accommodation via Kalman filtering. However, the simplifying assumptions used in the determination of the controller are less accurate than those implemented by Scheeres and Vinh or Hamilton. In particular, although motion of the chief spacecraft is assumed to proceed along a quasi-periodic Lissajous trajectory, one that is modeled via a linear approximation, the system matrix used to evaluate the optimal controller is, in fact, associated with the libration point rather than the actual nominal orbit. Although the controller appears to be successful, the resulting costs seem too high considering the fact that no velocity injection errors are included in the examples. An injection error in position, even a large one, is usually relatively simple to correct and requires minimal ΔV via LQR.

In an effort to evaluate the simplifying assumptions and, in contrast with the work done by Scheeres and Vinh [25], Hamilton [29], and Folta et al. [30], no simplifying assumptions are made in the present study about the form of the linear system. Hence, the LQR controller is formulated using the true time-varying dynamics associated with the reference path. This requires that the differential matrix Riccatti equation be numerically integrated, simultaneously, with the equations of motion associated with the nominal solution. The matrix solution is then used to compute the state feedback gain matrix. The controller derivation is based strictly on the optimality requirements established by the Euler-Lagrange theorem for time-varying systems as outlined in Bryson and Ho [32].

Dynamical Model of a Two-Spacecraft Formation in the CR3BP

There are a variety of ways to formulate the dynamics of a spacecraft (S/C) formation. In this study, the central spacecraft is termed "chief" while all other vehicles in the formation are denoted as "deputies". The motion of the chief S/C is described in terms of rotating coordinates relative to the barycenter of the system primaries (SEM system). In this frame, the rotating *x*-axis is directed from the Sun towards the Earth-Moon barycenter, as illustrated in Figure 1. The *z*-axis is normal to the plane of motion of the primaries, and the *y*-axis completes the right-handed triad. The general non-dimensional form of the equations of motion, relative to the system barycenter (B), are of the form

$$\ddot{x}(t) = f_x\left(x(t), y(t), z(t)\right) + 2\dot{y}(t) + x(t), \tag{1.1}$$

$$\ddot{y}(t) = f_y\left(x(t), y(t), z(t)\right) - 2\dot{x}(t) + y(t), \tag{1.2}$$

$$\ddot{z}(t) = f_z\left(x(t), y(t), z(t)\right), \tag{1.3}$$

where (x, y, z) denote the coordinates of the spacecraft relative to the barycenter B, and $\left(f_x, f_y, f_z\right)$ represents the net gravitational force vector acting on the vehicle. The force components are defined as

$$f_x(x, y, z) = -\frac{(1-\mu)}{r_1^3}(x+\mu) - \frac{\mu}{r_2^3}(x-1+\mu), \tag{1.4}$$

$$f_y(x, y, z) = -\left\{\frac{(1-\mu)}{r_1^3} + \frac{\mu}{r_2^3}\right\} y, \tag{1.5}$$

$$f_z(x, y, z) = -\left\{\frac{(1-\mu)}{r_1^3} + \frac{\mu}{r_2^3}\right\} z, \tag{1.6}$$

and r_1 and r_2 represent the radial distance from the spacecraft to the larger and smaller primary, respectively. In the Sun-Earth-Moon system, the Earth-Moon barycenter represents the smaller primary. The quantity μ is the non-dimensional mass parameter associated with the system. For the Sun-Earth-Moon system, $\mu \approx 3.0404 \times 10^{-6}$. During non-dimensionalization, the reference length is defined as the mean distance between the primaries. Since the Earth-Moon barycenter is roughly 4700 km away from the center of the Earth, the mean distance is assumed to be roughly equal to the semi-major axis of the Earth's orbit around the Sun, $l^* = 1$ au. The characteristic mass is the total mass of the system ($m^* = m_{sun} + \left(m_{earth} + m_{moon}\right)$), and the characteristic time is the inverse of the mean motion of the primaries, $t^* = (l^{*3}/(Gm^*))^{-1/2}$. In this study, the chief spacecraft dynamics are modeled using Equations (1.1)-(1.3) and the associated coordinates, relative to the barycenter, are defined as $\left(x_c, y_c, z_c\right)$.

For the deputy spacecraft, a more convenient choice of coordinates is one that describes the relative dynamics with respect to the chief. These relative dynamics may be modeled in terms of a variety of coordinates. For example, one could formulate the equations of motion in terms of relative spherical coordinates rather than cartesian coordinates. That is, the deputy S/C position can be expressed in terms of radial distance to the chief S/C (ρ), azimuth of the chief-deputy line as measured in the plane of motion of the primaries (ξ), and elevation relative to the plane (β). This formulation proves to be adequate when dealing with the two-dimensional CR3BP, where $\beta = 0^\circ$. However, the spherical formulation presents a series of modeling difficulties. Some are immediately apparent from the equations of motion and are analogous to gimbal lock when $\beta = 90^\circ$. Even if it is assumed that the operating range might temporarily be below this value, there are other issues associated with this formulation. The scale difference between the state variables (distance versus angular quantities) requires gain matrices whose elements differ by many orders of magnitude. This leads to computational difficulties during the numerical integration process.

Another setback is an unreasonable sensitivity to minute perturbations in the angular variables. These last two issues directly affect the effectiveness of any LQR approach. For instance, the LQR feedback controller may appear to be effective in dealing with distance perturbations but entirely inadequate in the presence of the slightest orientation errors.

Given the standard form of the CR3BP equations of motion in Equations (1.1)-(1.3), the simplest formulation corresponds to a set of cartesian coordinates (x_d, y_d, z_d), associated with the synodic rotating frame but measured relative to the chief spacecraft. Either actual relative coordinates or nonlinear error states with respect to some nominal motion may be used. For nominal motions of the deputy relative to the chief that can be represented analytically, such as formations fixed in either the rotating or inertial frames, cartesian coordinates relative to the chief spacecraft are sufficient. The controlled relative equations of motion associated with the deputy spacecraft dynamics are then defined by

$$\ddot{x}_d(t) = \Delta f_x(x_c, y_c, z_c, x_d, y_d, z_d) + 2\dot{y}_d(t) + x_d(t) + a_x(t), \tag{1.7}$$

$$\ddot{y}_d(t) = \Delta f_y(x_c, y_c, z_c, x_d, y_d, z_d) - 2\dot{x}_d(t) + y_d(t) + a_y(t), \tag{1.8}$$

$$\ddot{z}_d(t) = \Delta f_z(x_c, y_c, z_c, x_d, y_d, z_d) + a_z(t), \tag{1.9}$$

where a_x, a_y, and a_z denote the control accelerations along each direction and the differential gravitational forces are computed as

$$\begin{aligned} \Delta f_x &= f_x(x_c + x_d, y_c + y_d, z_c + z_d) - f_x(x_c, y_c, z_c), \\ \Delta f_y &= f_y(x_c + x_d, y_c + y_d, z_c + z_d) - f_y(x_c, y_c, z_c), \\ \Delta f_z &= f_z(x_c + x_d, y_c + y_d, z_c + z_d) - f_z(x_c, y_c, z_c). \end{aligned} \tag{1.10}$$

For a general time-varying reference solution defined by the state vector

$$\bar{x}(t)^\circ = \begin{bmatrix} x_d(t)^\circ & y_d(t)^\circ & z_d(t)^\circ & \dot{x}_d(t)^\circ & \dot{y}_d(t)^\circ & \dot{z}_d(t)^\circ \end{bmatrix}^T, \tag{1.11}$$

the linearized dynamics associated with Equations (1.7)-(1.9) are represented by a first order system of the form

$$\delta\dot{\bar{x}}(t) = A(t)\delta\bar{x}(t) + B(t)\delta\bar{u}(t). \tag{1.12}$$

The vector $\delta\bar{x}(t)$ denotes the perturbed state relative to the desired reference solution, $\bar{x}(t)^\circ$. Hence, the deputy state, at any time, can be represented by $\bar{x}(t) = \bar{x}(t)^\circ + \delta\bar{x}(t)$. The time varying linear system matrix, $A(t)$, is evaluated along the reference solution, $\bar{x}(t)^\circ$, that defines the desired formation configuration and is of the form

$$A(t) = \begin{bmatrix} 0 & 0 & 0 & 1 & 0 & 0 \\ 0 & 0 & 0 & 0 & 1 & 0 \\ 0 & 0 & 0 & 0 & 0 & 1 \\ \dfrac{\partial \Delta f_x}{\partial x_d} + 1 & \dfrac{\partial \Delta f_x}{\partial y_d} & \dfrac{\partial \Delta f_x}{\partial z_d} & 0 & 2 & 0 \\ \dfrac{\partial \Delta f_y}{\partial x_d} & \dfrac{\partial \Delta f_y}{\partial y_d} + 1 & \dfrac{\partial \Delta f_y}{\partial z_d} & -2 & 0 & 0 \\ \dfrac{\partial \Delta f_z}{\partial x_d} & \dfrac{\partial \Delta f_z}{\partial y_d} & \dfrac{\partial \Delta f_z}{\partial z_d} & 0 & 0 & 0 \end{bmatrix}. \tag{1.13}$$

The 6×3 matrix $B(t)$ in this case is constant and defined by $B = \begin{bmatrix} 0_{3\times3} & I_{3\times3} \end{bmatrix}^T$. Note that, even if the desired nominal motion is constant, the matrix $A(t)$ is time-varying because the partial derivative terms in Equation (1.13) depend explicitly on the path of the chief S/C, that is $\left(x_c(t), y_c(t), z_c(t)\right)$. These elements are periodic in nature since the chief is assumed to evolve along a halo orbit. The control input is defined by the vector $\bar{u}(t) = \begin{bmatrix} a_x(t) & a_y(t) & a_z(t) \end{bmatrix}^T$.

This formulation is effective, for instance, when the desired nominal motion corresponds to fixed distance and orientation in the rotating or inertial frames, both of which can be easily represented analytically. However, if the nominal motion is quasi-periodic, for instance, the solution must be stored and numerically approximated on demand during the integration procedure. In this study, quintic splines are used to model the nominal quasi-periodic orbit. Since there is some error introduced by this estimate, some difficulties may be encountered during the numerical integration process such as a decrease in computational speed or, at times, non-convergence. This problem is bypassed by modeling the dynamics in terms of the error relative to the nominal,

$$\begin{aligned} \ddot{e}_x(t) &= \left(\Delta f_x - \Delta f_x^{\circ}\right) + 2\dot{e}_y(t) + e_x(t) + \left(a_x - a_x^{\circ}\right), \\ \ddot{e}_y(t) &= \left(\Delta f_y - \Delta f_y^{\circ}\right) - 2\dot{e}_x(t) + e_y(t) + \left(a_y - a_y^{\circ}\right), \\ \ddot{e}_z(t) &= \left(\Delta f_z - \Delta f_z^{\circ}\right) + \left(a_z - a_z^{\circ}\right), \end{aligned} \tag{1.14}$$

where the superscript "o" implies that the differential gravity forces and control accelerations are evaluated along the nominal path of the deputy. The linear system matrix $A(t)$ associated with the system in Equation (1.14) is of the same form as that in Equation (1.13) but the partial derivative terms must be modified accordingly.

Nominal Formations

In this study, four types of nominal formations are considered for the chief-deputy line: fixed relative distance and orientation with respect to the rotating and inertial frames; quasi-periodic motion around a halo orbit; and, fixed radial distance with no orientation requirements. Any control strategy that relies on the linearized dynamics of the system, such as LQR, requires that a nominal formation keeping cost be initially determined. In the case of formation flight in the CR3BP, the question then becomes – is the baseline control effort required to achieve and maintain some desired configuration, physically reasonable? The following sections address this issue in detail.

Formations Fixed Relative to the CR3BP Rotating Frame

One possible type of formation corresponds to a configuration such that the relative distance between the chief spacecraft and the deputy is constant and the relative orientation of the chief-deputy line is fixed with respect to the rotating frame. Mathematically, this type of formation is described by a constant set of position elements for the deputy vehicle (all time derivatives relative to the rotating frame are zero along the nominal path). In order to apply LQR control, it is necessary to first identify the baseline cost associated with tracking the nominal state. If the position elements are to remain constant for all time, then, from Equations (1.7)-(1.9), the nominal formation keeping control accelerations (denoted by the superscript "∘") are defined by

$$a_x^{\circ} = -\left(\Delta f_x^{\circ} + x_d^{\circ}\right), \tag{1.15}$$

$$a_y^{\circ} = -\left(\Delta f_y^{\circ} + y_d^{\circ}\right), \tag{1.16}$$

$$a_z^\circ = -\Delta f_z^\circ. \tag{1.17}$$

To compute the cost incurred in maintaining the nominal formation over some prescribed period of time (Δt), it is necessary to numerically integrate both the chief and deputy equations of motion simultaneously. If the system is expressed in first order form, a total of 12 states are numerically integrated. If the state vector is augmented by one, and a new state $\Delta V(t)$ is introduced such that

$$\Delta \dot{V}(t) = \sqrt{\left(a_x^\circ\right)^2 + \left(a_y^\circ\right)^2 + \left(a_z^\circ\right)^2}, \tag{1.18}$$

then the total propulsive cost required to maintain the formation over a period of Δt time units is defined as the 13th state at time t.

The trajectory of the chief spacecraft is assumed to evolve along a natural halo orbit and completes one revolution in approximately six months. A single deputy spacecraft is located at a specific distance (ρ) and orientation (ξ, β) relative to the chief. This is defined as the baseline formation. The cost (ΔV) to maintain this formation fixed with respect to the rotating frame is determined over one revolution along the path of the chief spacecraft. The total cost associated with maintaining a variety of formations is illustrated in Figure 2. Three surfaces are displayed in this illustration. The narrower green surface corresponds to a halo orbit characterized by a 1.2×10^6 km out-of-plane amplitude (A_z), the intermediate blue contour is associated with an A_z of 700,000 km, and the wider red outline pertains to an A_z of 200,000 km. Each surface is associated with a formation defined by a 5000 km separation (ρ). The total cost (ΔV) is represented as a function of the azimuth (ξ) and elevation (β) of the chief-deputy line, as defined in Figure 1. For a nominal halo orbit (chief S/C) with an out-of-plane amplitude (A_z) of 200,000 kilometers, the formation keeping cost ranges between 10.8 m/sec ($\beta = 0^\circ$ and $\xi = 90^\circ$) and 26.9 m/sec ($\beta = 0^\circ$ and $\xi = 0^\circ$). Note that the surfaces displayed in Figure 2 exhibit two local minima, one at $\beta = 90^\circ + n\pi$ and the other at $(\xi, \beta) = (90^\circ + n\pi, 0^\circ)$, for $n = [0,1]$. Although the cost associated with these configurations is similar, they are not the same. In fact, a formation described by $(\xi, \beta) = (90^\circ, 0^\circ)$ is slightly less expensive. Figure 3 illustrates how these minimum-cost formations evolve relative to the rotating frame. It is apparent, from Figures 2 and 3, the formations that are orthogonal to the Sun-Earth-Moon line result in the lowest formation keeping costs for the particular segment of the halo family associated with the surfaces in Figure 2. The maximum cost case, $(\xi, \beta) = (0^\circ + n\pi, 0^\circ)$, then, corresponds to a formation that is always parallel to the Sun-Earth-Moon line. The net control acceleration levels for this particular configuration range between 1.45×10^{-6} and 2.66×10^{-6} m/sec^2, as noted from Figure 4. In contrast, for a halo orbit defined by A_z = 700,000 km, the cost ranges between 11.9 m/sec and 24.9 m/sec. For the maximum cost configuration, $(\xi, \beta) = (0^\circ + n\pi, 0^\circ)$, the acceleration level is anywhere between 1.23×10^{-6} m/sec^2 and 2.85×10^{-6} m/sec^2.

Along the highlighted segments of the halo families illustrated in Figure 5, the variation in the total cost required to maintain a 5000 km formation fixed in the rotating frame is illustrated in Figure 6. The cost variations displayed in Figure 6 include only members of the L_1 and L_2 halo families that have reached the critical amplitude, as highlighted in Figure 5. Beyond this point, the formation keeping cost increases rapidly to extremely prohibitive values, at least for a 5000 km formation. This is not unusual considering that, beyond this critical point, the perigee along the halo orbit collapses closer to the Earth. The bold lines in Figure 6 are associated with the L_2 halo family while the dashed lines pertain to the L_1 family. The blue and green lines are associated with the $(\xi, \beta) = (90^\circ, 0^\circ)$ and $\beta = 90^\circ$ minimum cost formations, respectively. The red lines are indicative of the maximum cost formation, $(\xi, \beta) = (0^\circ, 0^\circ)$. The pattern in Figure 6 indicates that the surfaces in Figure 2 change concavity when the A_z amplitude reaches a critical value of roughly 1.55×10^6 km. Hence, the $(\xi, \beta) = (90^\circ, 0^\circ)$ and $\beta = 90^\circ$ configurations, previously associated with the minimum cost formations, transition into maximum cost formations for A_z > 1.55x10^6

km. Similarly, what was previously the most costly configuration, $(\xi,\beta)=(0^\circ,0^\circ)$, now evolves into a global minimum for $A_z > 1.55\text{x}10^6$ km.

For most practical mission applications, the reference halo orbits of interest are likely to be in the range $A_z < 1.55\times10^6$ km. Otherwise, the nominal formation keeping cost may become prohibitive, at least for formations characterized by large relative separations between vehicles. Smaller formations with relative separations under 1 kilometer may still yield reasonable costs. Overall, the most cost effective formation configurations, ones that are fixed in the rotating frame, can be deduced from the illustration in Figure 6.

Formations Fixed Relative to the Inertial Frame

Let $\bar{r}_d$ denote the position vector of the deputy S/C relative to the chief S/C in terms of rotating coordinates (R). A formation that is fixed with respect to the inertial frame (I) must satisfy

$$ {}^I\dot{\bar{r}}_d = {}^R\dot{\bar{r}}_d + {}^I\bar{\omega}^R \times \bar{r}_d = \bar{0}, \tag{1.19}$$

$$ {}^I\ddot{\bar{r}}_d = {}^R\frac{d\left({}^I\dot{\bar{r}}_d\right)}{dt} + {}^I\bar{\omega}^R \times {}^I\dot{\bar{r}}_d = \bar{0}, \tag{1.20}$$

where ${}^I\bar{\omega}^R = n\hat{z}$, and n represents the rotation rate of the primaries about the barycenter. In non-dimensional time units, $n=1$. Equation (1.19) implies that the nominal velocities are defined by

$$ \dot{x}_d{}^\circ = ny_d{}^\circ, \tag{1.21}$$

$$ \dot{y}_d{}^\circ = -nx_d{}^\circ, \tag{1.22}$$

$$ \dot{z}_d{}^\circ = 0. \tag{1.23}$$

Hence, if the initial position is defined by (x_0, y_0, z_0), then the initial velocity may be computed from Equations (1.21)-(1.23) and the resulting analytical solution that describes the desired nominal motion is

$$ x_d{}^\circ(t) = x_0\cos nt + y_0\sin nt, \tag{1.24}$$

$$ y_d{}^\circ(t) = -x_0\sin nt + y_0\cos nt, \tag{1.25}$$

$$ z_d{}^\circ(t) = z_0. \tag{1.26}$$

Recall that the orientation variables ξ and β are measured relative to the rotating frame as defined in Figure 1. The inertial azimuth, $\xi_i(t)$, is defined as $\xi_i(t)=\xi(t)+\theta(t)$, where $\theta(t)$ represents the orientation of the rotating *x*-axis with respect to the inertial *X*-axis. Since all frames are assumed to be initially aligned, $\theta(0)=\theta_0=0^\circ$. Hence, for an inertially fixed configuration, the inertial orientation of the chief-deputy line is constant and characterized by $\xi_0+\theta_0=\xi_0$ and β_0. The subscript "0" implies the quantities are evaluated at $t=0$.

The formation constraints defined in Equations (1.19)-(1.20) require nominal control accelerations that overcome the net gravitational force acting on the deputy, i.e.,

$$ a_x{}^\circ = -\Delta f_x{}^\circ, \tag{1.27}$$

$$ a_y{}^\circ = -\Delta f_y{}^\circ, \tag{1.28}$$

$$ a_z{}^\circ = -\Delta f_z{}^\circ. \tag{1.29}$$

Unlike formations that are fixed relative to the rotating frame, Figure 7 reveals that the minimum and maximum costs, associated with an inertially fixed formation, depend only on the elevation with respect to the plane of motion of the primaries. For different reference halo orbits, the minimum and maximum costs

occur at different values of ξ_0 but are always associated with the same value of β_0 along the halo family. The maximum formation keeping cost is always associated with a formation that evolves in the plane of motion of the primaries for all time. The minimum cost, then, corresponds to a formation that is perpendicular to the plane of motion of the primaries as the chief S/C evolves along the halo orbit. Unlike in the previously considered formation, the overall characteristics of the surface in Figure 7 remain unaltered as the A_z amplitude of the reference halo orbit increases, as observed in Figure 8.

Center Manifold Formations

Howell and Barden [28] propose formations that take advantage of the structure of the center subspace near the reference halo orbit. In particular, formations that evolve along a two-dimensional torus that is known to envelop the halo orbit. For a reference halo orbit of period T characterized by a 200,000 km out-of-plane amplitude, one such sample surface is illustrated in Figures 9 and 10. Along the surface of the torus illustrated in Figure 9, the relative separation of the deputy spacecraft with respect to the chief ranges between 14,000 km and 58,000 km. Naturally, this represents an extremely large range and is only selected to aid the visualization process. The configuration can be designed to achieve relative distances of 14 meters to 58 meters instead. The colored spheres along the surface in Figure 9 represent 5 spacecraft. These spheres illustrate the motion that the vehicles experience longitudinally as the formation moves along the nominal halo orbit, as well as the winding motion as the formation revolves on the torus. Computation of this two-dimensional torus is a two step process. First, the monodromy matrix, $\Phi\left(T+t_0,t_0\right)$, associated with the reference halo orbit must be computed. This is accomplished by numerically integrating Equations (1.1)-(1.3), along with the matrix differential equation

$$\dot{\Phi}\left(t,t_0\right)=A\left(t\right)\Phi\left(t,t_0\right), \tag{1.30}$$

over one period of the reference orbit. Then, the eigenvectors of the monodromy matrix are computed. The majority of the halo family is comprised of unstable orbits, with the exception of a small range among the relatively large orbits. The unstable orbits have a four-dimensional center subspace. It is possible to select an initial perturbation that excites only one of the modes associated with the center eigenspace. The perturbation vector is then entirely contained within a specific subset of the center subspace. Howell and Barden first generate a linear version of a two-dimensional torus by propagating the predetermined initial perturbation using the solution to the linear system,

$$\delta\overline{x}\left(t\right)=\Phi\left(t,t_0\right)\delta\overline{x}\left(t_0\right). \tag{1.31}$$

As time progresses, the columns of the state transition matrix tend to align themselves with the unstable subspace. Hence, as the numerical error builds up, propagation of the initial perturbation vector, using Equation (1.31) over an extended length of time, yields inaccurate results. To circumvent this numerical difficulty, Howell and Barden use the projection theorem at the end of each revolution to project the final state back onto the center subspace. This "linear" torus serves as an initial guess to a two-level differential corrections process, described by Howell and Pernicka [33], that is used to generate the exact solution in the nonlinear system. In the present investigation, this is accomplished using software previously developed at Purdue University [34]. For a center manifold formation, the deputy spacecraft is assumed to evolve along this torus. LQR and nonlinear control techniques are implemented to track the nominal motion in the presence of injection and tracking errors. To accomplish this, it is necessary to find an analytical representation of the torus. Since an analytical solution is not available in the full nonlinear CR3BP, the differentially corrected torus is represented using quintic splines. Of course, motion along the torus represents a naturally occurring solution in the CR3BP. Hence, there is no nominal formation keeping cost associated with this type of configuration.

Formation Control

A simple test to determine the effectiveness of the available control strategies, in a multi-body regime, is to introduce both injection and tracking errors in the reference trajectory and assess the properties of the response. In this study, it is assumed that the reference trajectory of the chief vehicle is a three-dimensional, periodic halo orbit in the vicinity of the Sun-Earth-Moon L_1 point. The goal of the controller for the chief S/C is to accurately track the nominal halo orbit. In formation flight, the deputy spacecraft should then follow some prescribed nominal motion relative to the chief. The baseline motion for the deputy includes one natural and three non-natural but prescribed behaviors. Continuous control in response to injection and tracking errors is investigated here for all cases.

In designing an effective, practical controller for onboard S/C formation keeping, simplicity is the key. As de-centralized strategies, nonlinear and optimal control are both effective in maintaining a multi-spacecraft formation. Nonlinear control strategies, such as input or output feedback linearization, allow the designer to pre-specify the desired error dynamics. For time-varying systems, this leads to improved performance over linear control methods. Whether this improved performance comes at a lower or higher cost depends on the form of the dynamical model and the forces that must be overcome to achieve the desired response. The computational simplicity of this method is very appealing. However, this control approach also has its disadvantages. One of these disadvantages is that the methodology requires full-state feedback. Furthermore, as discussed by Chen et al. [35], an inherent flaw in this design approach is that the controller is more complex than the original system. In essence, this controller removes the natural dynamics and replaces them with the desired behavior. Although the approach is mathematically sound, physically incorporating such a controller on a spacecraft may be a daunting task. This is particularly true for highly complex nonlinear dynamics such as those associated with the CR3BP. Hence, if a linear controller can achieve the desired dynamics then it is usually recommended over nonlinear control, even when the nonlinear controller can yield far better response characteristics. Comparative performance evaluations are, thus, useful.

From a mathematical or computational perspective, optimal control is more complex than feedback linearization. Both the nonlinear and linear quadratic regulators (NQR and LQR) require that a two-point boundary value problem, with mixed boundary conditions, be solved. For a general time-varying nominal solution, computing the optimal controller gain matrix requires that the equations of motion be integrated first, forward in time, and the solution stored over the entire duration of the mission. Then, an NQR controller requires that the co-state equations be integrated backwards in time, from the nominal end state, to evaluate the controller gain matrix. If instead, an LQR controller is desired, integration of the co-states can be replaced by integration of the 6×6 matrix differential Riccatti equation. For systems that are invariant under time transformation, such as the CR3BP, this two-point boundary value problem can be reduced to an initial value problem, as demonstrated later. However, in either case, the gain matrix must still be stored for later use. Although this transformation simplifies the implementation of the controller in the CR3BP, ultimately a real formation flight mission will require that this analysis be performed in the general ephemeris model, where no assumptions are made about the motion of the primaries. Unlike the CR3BP, the ephemeris model is not invariant under time transformation. Hence, implementing a quadratic regulator in the ephemeris model still requires solution of a two-point boundary value problem.

Both the nonlinear and linear quadratic regulators are more computationally intense in comparison to input/output feedback linearization. In the available literature, the more commonly encountered of these methods is the linear quadratic regulator. However, it should be noted that the LQR controller is only optimal for the linear system dynamics. For a time-varying system, there is no guarantee that the controller

will be successful over a wide range of operating conditions in the nonlinear model, or that it will result in a reasonable or "optimal" cost. In this study, linear optimal control, input feedback linearization (IFL), and output (or partial) feedback linearization are all applied to the formation keeping problem near the libration points in the CR3BP. The IFL and LQR controllers prove to be effective in maintaining the relative distance and orientation of the formation at a reasonable cost. Though both the IFL and LQR controllers yield similar response characteristics, this study demonstrates that the IFL controller is the most cost effective. The output feedback controller can lead to a similar response at a much lower cost, depending on the relative formation configuration that is considered. All three controllers respond well to both position and velocity injection errors.

Linear Quadratic Regulator for Time-Varying Systems

Consider a general nonlinear vector field of the form

$$\dot{\bar{x}}(t) = \bar{f}\left(\bar{x}(t), \bar{u}(t)\right), \tag{1.32}$$

where $\bar{x} \in \mathbb{R}^n$ is the state vector at time t, $\dot{\bar{x}}$ represents the time derivative of $\bar{x}$, $\bar{u} \in \mathbb{R}^{n/2}$ is defined as the control acceleration vector, and $\bar{f} : U \to \mathbb{R}^n$ is a smooth function defined on some subset $U \subseteq \mathbb{R}^n$. Let $\bar{x}^\circ(t)$ denote some reference motion that satisfies the system in Equation (1.32) and $\bar{u}^\circ(t)$ represent the control effort required to sustain $\bar{x}^\circ(t)$. Linearization about this reference solution yields a system of the form

$$\delta\dot{\bar{x}}(t) = A(t)\delta\bar{x}(t) + B(t)\delta\bar{u}(t), \tag{1.33}$$

where $\delta\bar{x}$ and $\delta\bar{u}$ represent perturbations relative to $\bar{x}^\circ(t)$ and $\bar{u}^\circ(t)$, respectively. Consider a general quadratic cost function of the form

$$\min J = \frac{1}{2}\int_{t_0}^{t_f}\left(\delta\bar{x}(t)^T Q\delta\bar{x}(t) + \delta\bar{u}(t)^T R\delta\bar{u}(t)\right)dt, \tag{1.34}$$

subject to the system in Equation (1.33) with initial conditions $\delta\bar{x}(t_0) = \delta\bar{x}_0$. The matrices Q and R represent the weighting on the state error and control effort, respectively, and are both symmetric positive definite. For simplicity, let Q and R be diagonal matrices. This implies that the individual state variable errors, and control accelerations, are decoupled. Since the cost function can be scaled by any constant without affecting the results, only the relative magnitudes of the elements of Q and R are important. Hence, in this study R denotes the 3×3 identity matrix and Q, scaled relative to R, is given by $Q = diag\left(Q_p, Q_p, Q_p, Q_v, Q_v, Q_v\right)$ where Q_p and Q_v are the position and velocity weights, respectively. The structure of this matrix places equal weighting on each position error, and each velocity error.

As outlined in Bryson and Ho [32], application of the Euler Lagrange theorem to the system in Equations (1.34) and (1.33) yields the following optimality requirements,

$$\dot{\bar{\lambda}}(t) = -Q\bar{x}(t) - A(t)^T\bar{\lambda}(t);\ \ \bar{\lambda}(t_f) = \bar{0}, \tag{1.35}$$

$$\bar{u} = -R^{-1}B(t)^T\bar{\lambda}(t). \tag{1.36}$$

Consider a state feedback controller by defining $\bar{\lambda}(t) = P(t)\delta\bar{x}(t)$. Substitution of this transformation into Equation (1.35) yields the following Riccatti matrix differential equation,

$$\dot{P}(t) = -A(t)^T P(t) - P(t)A(t) + P(t)B(t)R^{-1}B(t)^T P(t) - Q, \tag{1.37}$$

subject to $P(t_f) = 0_{6\times 6}$. Equations (1.37) and (1.7)-(1.9), or (1.14), represent a two point boundary value problem with 42 first order ordinary differential equations. Obtaining an exact solution to this equation is numerically inconvenient because it requires that the reference trajectory be integrated first forward in time from t_0 to t_f to evaluate $A(t)$ before integrating Equation (1.37) backwards from t_f to t_0. However, this difficulty can be avoided by exploiting the time invariance properties associated with the flow in the CR3BP. Consider the following time transformation,

$$\tau = t_f - t, \tag{1.38}$$

$$\frac{d}{dt} = -\frac{d}{d\tau}. \tag{1.39}$$

Since the linear system Equation (1.33) models the behavior for all time, positive or negative, introduce the following coordinate transformation,

$$z(\tau) = Gx(t), \tag{1.40}$$

where G denotes a constant non-singular matrix. For the free response ($\bar{u}(t) = \bar{0}$) the transformed state must also satisfy the differential equations,

$$\begin{aligned} \frac{dz(\tau)}{d\tau} &= A(\tau)z(\tau), \\ -\frac{d(G\bar{x}(t))}{dt} &= A(t_f - t)G\bar{x}(t), \\ \frac{d\bar{x}(t)}{dt} &= -G^{-1}A(t_f - t)G\bar{x}(t) = A(t)\bar{x}(t). \end{aligned}$$

Hence,

$$A(t) = -G^{-1}A(t_f - t)G. \tag{1.41}$$

But, Equation (1.41) must be satisfied for all time which further implies that

$$\begin{aligned} A(t_f - t) &= -G^{-1}A(t_f - (t_f - t))G = -G^{-1}A(t)G, \\ A(t) &= -GA(t_f - t)G^{-1}. \end{aligned} \tag{1.42}$$

For both Equations (1.41) and (1.42) to be satisfied, the matrix G must posses some special properties. In particular, $G^{-1} = G$, $G^2 = I$, but $G \neq I$. Since G must be a diagonal matrix to satisfy these conditions it must also satisfy

$$G = G^T = G^{-1} = G^{-T}. \tag{1.43}$$

The diagonal matrix $G_{jj} = (-1)^{j-1}$ satisfies all of the stated requirements.

Substitution of the time transformation defined by Equations (1.38) and (1.42) into (1.37) yields

$$-\frac{dS(\tau)}{d\tau} = A(\tau)^T S(\tau) + S(\tau)A(\tau) + S(\tau)\tilde{B}(\tau)R^{-1}\tilde{B}(\tau)^T S(\tau) - \tilde{Q} \tag{1.44}$$

where,

$$S(\tau) = G^{-1}P(t_f - \tau)G, \tag{1.45}$$

$$\tilde{B}(\tau) = G^{-1}B(t_f - \tau), \tag{1.46}$$

$$\tilde{Q} = G^{-1}QG. \tag{1.47}$$

The terminal boundary condition $P(t_f) = 0$ implies that when $\tau = 0$, $S(0) = 0$. Since Equation (1.44) must be satisfied for all time, let $\tau = t$ and then solve the equation,

$$\dot{S}(t) = -A(t)^T S(t) - S(t)A(t) - S(t)\tilde{B}(t)R^{-1}\tilde{B}(t)^T S(t) + \tilde{Q} \tag{1.48}$$

with $S(0) = 0$. Equation (1.48) can be numerically integrated to time t_f along with the nonlinear equations of motion (1.32). Then, using Equation (1.45),

$$P(t_f - t) = GS(t)G^{-1} = G^{-1}S(t)G. \tag{1.49}$$

This yields the controller gain matrix

$$K(t_f - t) = -R^{-1}B(t)^T S(t)G. \tag{1.50}$$

The process of implementing the linear controller in the nonlinear model is divided into two steps. In the first step, the nonlinear system described by Equation (1.32) is numerically integrated along with the matrix differential equation in Equation (1.48). These equations are subject to $\bar{x}(t_0) = \bar{x}_0$ and $S(t_0) = 0$, respectively. The results are used to determine $K(t)$ which is stored, along with the corresponding time, for later implementation. The second step is to numerically integrate the perturbed nonlinear equations and, at each time step, apply the control accelerations associated with the corresponding $K(t)$ matrix. The integration step size is determined by the first integration since the gain matrix elements are accessed from memory at each time.

It is not uncommon that, in adding an LQR controller to a time-varying system, the linearized dynamics are oversimplified by letting $\dot{P}(t) = 0$ in Equation (1.37). Then, computing the gain matrix reduces to solving the algebraic Riccatti equation at each point during the integration, each time evaluating Equation (1.37) with the corresponding matrix, $A(t)$. This approximate approach is frequently implemented and successful – though the theoretical reason for success may not be clear. In the CR3BP, the $A(t)$ matrix associated with a halo orbit is periodic, $A(t) = A(t+T)$. If $A(t)$ were constant, the differential equation in Equation (1.37) would converge to a constant matrix P. Hence, in practice, it is only necessary to solve for the constant steady state solution as defined by the algebraic Riccatti equation. When the reference solution is periodic, the differential Riccatti equation converges on a periodic matrix $P(t) = P(t+T)$. However, if the elements of Q are sufficiently large, the amplitude of the elements of the "steady state" solution are so large that the oscillations induced by $A(t)$ become negligible, at least in the CR3BP. Hence, solving the algebraic Riccatti equation at each time step, with the corresponding matrix $A(t)$, yields a solution that is close, but not exactly equal, to the true $P(t)$ matrix determined from Equation (1.37). Folta, Carpenter, and Wagner [30] further simplify the solution process by assuming $A(t)$ to be the constant linear system matrix associated with the libration point. In their study, the reference orbit around the equilibrium point is small in comparison to those considered here. Hence, they solve the algebraic Riccatti equation using the constant system matrix associated with the equilibrium point. For such a small orbit, the periodic deviations of the actual $A(t)$ matrix, relative to the constant matrix associated with the libration point, are also small. Thus, the LQR controller may still yield reasonable performance, assuming large gains. Even though using the approximate system matrix may yield reasonable results on a case by case basis, if a generally accurate

control approach is sought, then solving the differential Riccatti equation is the mathematically solid approach.

Input Feedback Linearization

Feedback linearization, as discussed in Slotine and Li [36], is a mathematically simple nonlinear control strategy that allows the designer to specify the desired response characteristics. For instance, consider a scalar differential equation of the form

$$\dot{\alpha}(t) = h(\alpha(t)) + \upsilon(t), \tag{1.51}$$

where $\alpha(t)$ represents the state at time t. In input feedback linearization, the control $\upsilon(t)$ is selected such that

$$\upsilon(t) = -h(\alpha(t)) + \tilde{\upsilon}(t). \tag{1.52}$$

The control acceleration, $\tilde{\upsilon}(t)$, in Equation (1.52) is designed to be representative of the desired nominal motion, $\alpha^{\circ}(t)$. For a critically damped response,

$$\tilde{\upsilon}(t) = \ddot{\alpha}^{\circ} - 2\omega_n\left(\dot{\alpha} - \dot{\alpha}^{\circ}\right) - \omega_n^{\,2}\left(\alpha - \alpha^{\circ}\right). \tag{1.53}$$

Any form of feedback linearization requires full-state feedback, one of the disadvantages of the approach. However, for formation flight, if the relative states are available, this method can be a powerful tool. Consider the controlled CR3BP equations of motion from Equations (1.7)-(1.9). It is possible to select a_x, a_y, and a_z such that each state follows a critically damped response that meets some prescribed settling time requirement. The individual response of each state can be decoupled by choosing control accelerations of the form,

$$a_x = \ddot{x}_d^{\,\circ} - 2\omega_n\left(\dot{x} - \dot{x}_d^{\,\circ}\right) - \omega_n^{\,2}\left(x - x_d^{\,\circ}\right) - \left(\Delta f_x + 2\dot{y}_d + x_d\right), \tag{1.54}$$

$$a_y = \ddot{y}_d^{\,\circ} - 2\omega_n\left(\dot{y} - \dot{y}_d^{\,\circ}\right) - \omega_n^{\,2}\left(y - y_d^{\,\circ}\right) - \left(\Delta f_y - 2\dot{x}_d + y_d\right), \tag{1.55}$$

$$a_z = \ddot{z}_d^{\,\circ} - 2\omega_n\left(\dot{z} - \dot{z}_d^{\,\circ}\right) - \omega_n^{\,2}\left(z - z_d^{\,\circ}\right) - \Delta f_z. \tag{1.56}$$

In this study, an acceptable response is one that reaches the desired solution in less than a day. A non-dimensional angular frequency (ω_n) of at least 1000 meets this requirement. It should be noted that decoupling the states is not necessarily the "optimal" solution, it is simply a way to accomplish the task. The feasibility of this control approach must be determined numerically by evaluating Equations (1.54)-(1.56) to determine if the total cost is physically reasonable. Furthermore, this approach is useful when the formation requires that both distance and orientation be completely specified in time. However, in formation flight applications, it may not be necessary to track each state individually. If the formation only requires that relative distance be specified then output (or partial) feedback linearization is better suited for the task.

Output Feedback Linearization

Output feedback linearization also requires full-state feedback. However, the controller design is much less constrained than input feedback linearization and it usually yields a lower total cost. Let the radial distance, between the deputy and chief spacecraft, and the associated radial rate be specified as the measured output. Then, reformulate the system in Equations (1.7)-(1.9) in terms of the relative radius vector, $\bar{r}$.

$$\ddot{\bar{r}}(t) = \bar{f}\left(\bar{r}(t)\right) + 2J\dot{\bar{r}}(t) + K\bar{r}(t) + \bar{u}(t) \tag{1.57}$$

Here, the 3×3 matrices J and K are defined as

$$J=\begin{bmatrix}0 & 1 & 0\\ -1 & 0 & 0\\ 0 & 0 & 0\end{bmatrix}, \tag{1.58}$$

$$K=\begin{bmatrix}1 & 0 & 0\\ 0 & 1 & 0\\ 0 & 0 & 0\end{bmatrix}. \tag{1.59}$$

Define the measured system output as

$$y=\begin{bmatrix}r\\ \dot{r}\end{bmatrix}, \tag{1.60}$$

where $r=\left(\bar{r}^T\bar{r}\right)^{1/2}$ denotes the separation, or range, between the chief and deputy spacecrafts and $\dot{r}$ represents the range rate. In output feedback linearization, the measured output is differentiated *q* times until the control vector appears explicitly. Then, the system is said to be of relative degree *q*. The goal, then, is to determine $\bar{u}(t)$ that yields the desired output response defined by $y=\begin{bmatrix}r_0 & 0\end{bmatrix}^T$. Differentiating (1.60) once with respect to time yields,

$$\begin{bmatrix}\dot{r}\\ \ddot{r}\end{bmatrix}=\begin{bmatrix}\left(\bar{r}^T\bar{r}\right)^{-\frac{1}{2}}\left(\bar{r}^T\dot{\bar{r}}\right)\\ \left(\bar{r}^T\bar{r}\right)^{-\frac{1}{2}}\left(\dot{\bar{r}}^T\dot{\bar{r}}+\bar{r}^T\ddot{\bar{r}}\right)-\left(\bar{r}^T\bar{r}\right)^{-\frac{3}{2}}\left(\bar{r}^T\dot{\bar{r}}\right)^2\end{bmatrix}. \tag{1.61}$$

In Equation (1.61) the control appears through the $\ddot{\bar{r}}$ term. The desired response should satisfy $\ddot{r}=g(r)$ subject to $\dot{r}=0$. It is possible to substitute the vector in Equation (1.57) into Equation (1.61) and, after some vector manipulation, solve for the control law that achieves the desired output response

$$\bar{u}(t)=\left(\frac{g(r)}{r}-\frac{\dot{\bar{r}}^T\dot{\bar{r}}}{r^2}\right)\bar{r}-\left(\bar{f}(\bar{r})+2J\dot{\bar{r}}+K\bar{r}\right). \tag{1.62}$$

Observe that the last term in Equation (1.62) serves to, once again, cancel the natural dynamics of the problem while the first two terms enforce the desired response. For the purpose of distance tracking, a critically damped response would require that

$$g(r)=\ddot{r}^{\circ}-2\omega_n\left(\dot{r}-\dot{r}^{\circ}\right)-\omega_n{}^2\left(r-r^{\circ}\right), \tag{1.63}$$

where the superscript "$\circ$" implies that the quantity is evaluated along the reference path. A distinct advantage of feedback linearization over LQR, is the ability to pre-specify the error dynamics. If the weighting matrices of the LQR controller are chosen as diagonal, there is always an overshoot associated with the response. This can increase the cost because, as the solution moves farther away from the nominal, the controller has to exert more effort to drive it back to the desired state within the specified time frame. The overshoot and settling time can be reduced by choosing sufficiently large elements for the state weighting matrix *Q*, relative to those of *R*. In particular, the weights associated with the position errors should be very large and many orders of magnitude greater than the weights on the velocity errors. Essentially, this reduces the control accelerations to a nearly impulsive maneuver. The problem then becomes, finding the gain matrices that force the LQR controller to produce a nearly critically damped response (e.g. no overshoot). There is no simple way to accomplish this analytically and ensure that the response will follow critically damped dynamics under any perturbation. However, if the weights are sufficiently large, it is possible to attain a response that is similar in character to critically damped

dynamics, at least in terms of overshoot. Here, the feedback linearization approach is designed to yield a truly critically damped response while the LQR will usually exhibit some degree of oscillations before reaching the desired nominal state.

RESULTS

In general, the chief spacecraft evolves along an unstable halo orbit and the desired baseline motion of the deputy does not always correspond to a naturally occurring solution. Hence, if left uncontrolled, the deputy spacecraft would quickly leave the vicinity of the chief in its orbit. For instance, let the desired baseline motion correspond to a formation that is fixed with respect to the rotating frame, at a relative distance of 5000 km, and a reference halo orbit of $A_z = 200,000$ km. In the absence of control inputs, the natural response of the system would place the deputy anywhere between 1.6 km and 5.5 km away from the initial position within a day, depending on the configuration considered. Subsequently, divergence is exponential; within 8 days the deputy would be 100 km away. The impact is, of course, less noticeable for smaller formations. For instance, at most, an uncontrolled 50 meter formation will diverge by 1 meter within 6 days. The rate of divergence is lowest for the minimum-cost formations and highest for the maximum-cost formations. The inertially fixed formations tend to diverge at a faster rate. A 5000 km formation fixed relative to the inertial frame can diverge between 2.5 and 4.5 km from its initial distance within a day. Within 8 days, the deputy will have diverged from its nominal path by almost 200 km. A 50 meter formation, on the other hand, would diverge at most by 1 meter within 4.5 days, depending on the formation orientation. This suggests that, if the formation tolerances are not too constrained, a discrete control approach may be sufficient for small formations. However, if the configuration constraints are tight and the nominal vehicle separations are relatively large, continuous control will likely be required. This is particularly true if the desired nominal motion is not representative of the natural flow of the system.

Formations Fixed Relative to the Rotating Frame

The LQR and input feedback linearization methods previously described are applied here to a 5000 km two-spacecraft formation fixed relative to the rotating frame. Both methods can be successfully applied to either the chief spacecraft orbit, described by Equations (1.1)-(1.3), or the deputy dynamics outlined in Equations (1.7)-(1.9). In particular, the line defining the formation is commanded to track the rotating *y*-axis at all times. As mentioned previously, this type of formation represents the most cost effective baseline configuration. Figures 11 and 12 illustrate the response to an injection error defined by $\delta\bar{r} = (7, -5, 3.5)$ km and $\delta\dot{\bar{r}} = (1, -1, 1)$ m/sec . For the LQR response, each figure lists the cost to maintain the baseline configuration alone, ΔV_{NOM} , as well as the total cost, $\Delta V_{LQR} = \Delta V_{NOM} + \Delta V_{\text{correction}}$, that is necessary to also correct the initial injection error. Thus, these values represent the propulsive cost required to maintain the formation over one revolution of the reference halo orbit. The top two plots in Figures 11 and 12 illustrate the response of the error dynamics in each state to the LQR controller. The response in Figure 11 is associated with a weighting matrix defined by $Q_p = 10^{10}$ and $Q_v = 10^5$. The settling time of the response is significantly improved by increasing the position error weight to $Q_p = 10^{12}$, as reflected in Figure 12. In contrast, the two plots at the bottom in Figures 11 and 12 illustrate the error response corresponding to each state for a controller based on Input Feedback Linearization (IFL), as represented by Equations (1.54)-(1.56), for $\omega_n = 400$ and $\omega_n = 1250$, respectively. As noted on these Figures, both controllers yield good tracking characteristics at essentially the same cost. Accordingly, the acceleration histories are almost identical and promptly converge onto the nominal acceleration required to maintain a formation fixed in the rotating frame. Numerical trials indicate that, for the selected controller parameters, the IFL controller is consistently less costly than the LQR controller, though only by a small amount, at most 1-2 m/sec. Furthermore, the response associated with the LQR controller exhibits some small

oscillations about the reference while the net error settles to zero. The IFL controller is consistent with a critically damped response, as stipulated by the original formulation. In both cases, the formation reaches the desired nominal configuration to within 1 meter in roughly 19 hours for the case illustrated in Figure 12. The similarities between the results are not surprising considering that, for the LQR approach, the state weighting matrix Q is selected as diagonal. Hence, the state errors are decoupled from each other. This is the same premise behind the IFL controller design as formulated in Equations (1.54)-(1.56).

Although the results in Figures 11 and 12 reflect only the response to initial injection errors, the methodology can be extended to accomplish reconfigurations during flight. For instance, suppose the formation must reconfigure its relative separation every 20 days by 10 km. Application of the LQR approach with $Q_p = 10^{12}$ and $Q_v = 10^5$ yields the response presented in Figure 13. Each reconfiguration is accomplished by a net 1.92 m/sec correction above the required nominal formation keeping cost, ΔV_{NOM}. The reconfiguration can also be accomplished using the IFL controller.

The sample formations presented here, as well as the injection errors that are considered, are large in comparison to those presented by most authors [7-24]. Most of these cases involve separations that range between 10 meters to 1 km and the injection errors are scaled accordingly. In the present study, large formations are desirable to determine the operating range of these controllers. Both the LQR and IFL controllers will respond in a similar form, and yield similar costs, even to the most absurd perturbations but, of course, at an equally absurd cost. Numerical analysis indicates that changing the size of the formation by one order of magnitude impacts the nominal cost by the same order of magnitude. For instance, a 10 meter formation requires a nominal cost of 2.538×10^{-5} m/sec, over one period of the reference halo orbit, while a 1×10^5 meter formation requires 2.166×10^{-1} m/sec. The total cost increased by 4 orders of magnitude along with the stipulated separation distance, but it is still quite small. Since the net cost is so low, the problem is then in the delivery. Even with electric propulsion, the thrust level required to maintain these formations is extremely low. For instance, a minimum cost 100-meter formation has nominal acceleration requirements defined by $0.86\times10^{-11} < |\bar{u}_{NOM}| < 2\times10^{-11}$ m/sec^2. For a 2000 kg spacecraft, this is equivalent $1.7\times10^{-5} < F < 4\times10^{-5}$ mN. A 5000 km minimum-cost formation, on the other hand, would require nominal thrust levels ranging between $0.86 < F < 2.1$ mN. As detailed in the Technology Validation Report on the NSTAR Engine [37] used in DS-1, the minimum thrust level achievable by the ion-engine is 20mN. If the results presented here pertained to a two-body regime, this would appear to suggest that larger formations are best serviced by continuous control while smaller formations can be designed around the classical discrete station-keeping approach. However, the chaotic nature of the CR3BP is characterized by extreme sensitivity to small perturbations. That is, the smallest deviation from the nominal path results in exponential divergence. Hence, continuous control may still be required, particularly for non-natural formations.

Formations Fixed in the Inertial Frame

Formations fixed relative to inertial directions are just as effectively controlled by either of the two methods described above. Once again, let the reference halo orbit be characterized by $A_z = 200{,}000$ km. Assume that the deputy is to follow the chief spacecraft as it evolves along the reference halo orbit over one revolution. Then, the propulsive cost required to maintain the formation, one that is fixed with respect to the inertial frame, ranges from 12.7 m/sec to 19.7 m/sec, depending on the desired configuration. The minimum cost formation corresponds to the case when the formation line is aligned with the inertial *Z*-axis. That is, as the chief spacecraft moves along the reference halo orbit, the deputy is always located directly above, along the inertial *Z*-axis. A sample response to an initial injection error of $\delta\bar{r} = (7, -5, 3.5)$ km and $\delta\dot{\bar{r}} = (1, -1, 1)$ m/sec is presented in Figure 14. Once again, both methods yield essentially the same

response for an almost identical cost, but the IFL method is computationally simple to implement compared to the LQR approach. In contrast, the maximum cost is associated with a formation that remains aligned with the inertial *X*-axis.

Radial Distance Tracking With No Orientation Requirements

Some formations might require only that the chief and deputy spacecraft maintain some constant distance at all times, without constraining their relative orientation in any frame. For this type of formation keeping, the only "nominal" variable is the radial separation between each spacecraft. This is assumed to be the only "measured" variable although full state feedback is still required to compute the control input. Consider, then, the output feedback controller defined in Equation (1.62). The reference halo orbit still corresponds to a 200,000 km out-of-plane amplitude. In this type of approach, a nominal state vector is not defined. To verify that the controller can maintain a constant distance, let the "nominal" control effort represent the input required to maintain the formation at its starting distance, as defined by the initial conditions. During this test, no injection errors are added. For a set of initial conditions of the form $(x_d, y_d, z_d, 0, 0, 0)$, this controller yields the same nominal cost determined by the surface in Figure 2. For a 5000 km formation relative to a 200,000 km halo orbit, the nominal cost varies between 10.8 m/sec and 26.9 m/sec. Once the controller's ability to maintain the nominal formation is assessed, its effectiveness in the presence of injection errors is determined. For the same injection error considered with the IFL controller, maintaining a constant relative distance of 5000 km relative to the chief spacecraft requires between 14.9 m/sec and 22.4 m/sec, depending on the initial alignment of the formation. Of course, in this case, the state of the deputy with respect to the chief is not fixed relative to any particular reference direction, as seen from the bottom two plots in Figure 15. The controller is only designed to achieve a constant relative distance between the two spacecraft, in this case 5000 km. For a natural frequency of $\omega_n = 1250$, the critically damped response characteristics of the radial distance are essentially the same as those previously presented for each individual state via the IFL controller, as observed from the top two illustrations in Figure 15.

Formations Evolving Along the Center Manifold

A formation evolving along the center manifold, associated with the reference halo orbit, is characterized by bounded motion. That is, the motion of the deputy relative to the chief is quasi-periodic. Motion along the center manifold is a function of two frequencies. One of these frequencies is associated with the period of the reference orbit and the associated modes are tangent to nearby periodic solutions. The second frequency characterizes the winding motion along the surface of a torus that envelopes the halo orbit, as discussed by Howell and Barden [26]. If the initial state of the deputy is selected such that only the modes associated with the second frequency are excited, the resulting motion, over 200 orbital periods, is illustrated in Figure 9. The formations considered by Howell and Barden [27-28] evolved along a surface similar to that in Figure 9.

Since this type of motion is part of the natural phase space corresponding to periodic halo orbits, no nominal cost is required to maintain a formation such that the deputy S/C evolves along the torus, $\Delta V_{NOM} = 0$. As previously determined, both the LQR and the IFL controllers are effective in counteracting injection errors in this case as well. The correction costs for both approaches, is on the same order of magnitude as the velocity injection error. For an injection error defined by $\delta\bar{r} = (7, -5, 3.5)$ km and $\delta\dot{\bar{r}} = \delta\bar{v} = (1, -1, 1)$ m/sec, the LQR controller requires a 3.91 m/sec correction, assuming $Q_p = 10^{12}$ and $Q_v = 10^5$. The IFL controller, with requires 3.66 m/sec to correct the injection error. The associated error response is presented in Figure 16.

Of course, if the deputy spacecraft motion is quasi-periodic relative to the chief, such as the motion on the torus, the relative separation between the two spacecraft will not be naturally constant. The radial distance between the deputy and chief S/C for a relatively small formation is illustrated in Figure 17. If the relative separation of the two spacecraft is less critical than their relative orientation, Barden and Howell [28] have demonstrated that maintaining multiple spacecraft on a formation plane is a feasible configuration in terms of cost. Further study of natural formations along the center manifold is a future topic of interest.

Response to Tracking Errors

The formation dynamics, as developed in this study, only incorporate control inputs. No disturbance inputs are included in the mathematical model. Hence, disturbance accommodation is not implemented in the development of the controllers considered here. Theoretically, there is no guarantee that either the LQR or IFL controllers, as presently formulated, will maintain the formation in the presence of disturbances. Even if both controllers are successful at tracking the desired formation, the cost required to compensate for disturbances may be prohibitive. However, it is still compelling to investigate, numerically, how these two controllers perform in the presence of tracking errors along the trajectory.

Considering that the nominal acceleration levels required for formation keeping are so small, some of these tracking errors may be introduced by the propulsion system itself. Delivering such small acceleration levels accurately is difficult because the error introduced by the hardware may be on the same order of magnitude as the required control input, if not greater. Recall the case of the inertially fixed formation previously discussed. Suppose that, at each step along the trajectory, tracking errors are introduced to the numerically determined state vector. Let the standard deviations in position and velocity be characterized by 1 meter and 0.01 m/sec, respectively. These values are large considering that the automated formation flight systems on TPF are expected to be accurate to within centimeters in position and millimeters per second on range rate. The associated response is presented in Figure 18. As predicted, the formation keeping cost is considerably higher. However, it is interesting to note that the IFL controller performs significantly better than the LQR controller in the presence of tracking disturbances. That is in comparison to the previous case where the performance of both controllers was equivalent in response to injection errors. Naturally, for smaller tracking errors, characterized by 1 cm and 1 mm/sec standard deviations, both control methodologies yield more reasonable costs but the IFL controller still performs significantly better than the LQR approach as noted from Figure 19.

CONCLUSION

Increased interest in formation flight near the libration points of the Sun-Earth-Moon system has motivated a number of studies on the type of control required to maintain a prescribed formation in this highly sensitive region of space. However, most of the available literature on formation flight pertains to formations near the Earth, where a two-body model is appropriate. The first part of this study presents a survey of some of the work done to date on formation flight in the two-body model and how the control strategies previously implemented in that system perform in the rich phase space of the CR3BP. In this regime, non-naturally occurring formations, such as those that remain fixed relative to either the rotating or inertial frames, will likely require continuous control for precise tracking. Whether a continuous or discrete control approach is necessary depends on the relative separation of each spacecraft in the formation, with respect to the chief. Larger formations, on the order of 5000 km, will likely require continuous control for precise tracking. However, if the separation between the chief and deputy spacecraft is on the order of hundreds of meters, a discrete control approach may later prove to be sufficient, though further study into this matter is necessary. A study on the nominal formation keeping costs required to maintain these types of

configurations is also presented. The results indicate that for reference halo orbits that are below a critical out-of-plane amplitude, the formation keeping costs are miniscule, even for relative separations of 5000 km. Though LQR and nonlinear control techniques can be designed to yield a similar response in the presence of injection errors, the formation keeping cost appears to be consistently lower via nonlinear control. This trend is most noticeable when tracking errors are introduced into the system.

ACKNOWLEDGMENTS

The authors would like to extend their gratitude to Professor Mario Rotea of Purdue University for valuable discussions throughout this research effort. This research was carried out at Purdue University and was partially supported under Contract Number NAG5-11839 from the National Aeronautics and Space Administration.

REFERENCES

1. Space Based Observatories. [online] Available at http://origins.jpl.nasa.gov/missions/sbobs.html.

2. Space Technology-3 Homepage. [online] Available at http://planetquest.jpl.nasa.gov/StarLight/starlight_index.html

3. Terrestrial Planet Finder Book. [online] Available at http://planetquest.jpl.nasa.gov/TPF/tpf_book/index.html, May 1999.

4. Terrestrial Planet Finder Homepage. [online] Available at http://planetquest.jpl.nasa.gov/TPF/tpf_index.html.

5. Planet Imager Homepage. [online] Available at http://origins.jpl.nasa.gov/missions/pi.html.

6. Life Finder Homepage. [online] Available at http://origins.jpl.nasa.gov/missions/lf.html.

7. R.H. Vassar and R.B. Sherwood, "Formationkeeping for a Pair of Satellites in a Circular Orbit," *Journal of Guidance, Control, and Dynamics*, Vol. 8, Mar.-Apr. 1985, pp. 235-242.

8. D.C. Redding, N.J. Adams, and E.T. Kubiak, "Linear-Quadratic Stationkeeping for the STS Orbiter," *Journal of Guidance, Control, and Dynamics*, Vol. 12, Mar.-Apr. 1989, pp. 248-255.

9. Y. Ulybyshev, "Long-Term Formation Keeping of Satellite Constellation Using Linear Quadratic Controller," *Journal of Guidance, Control, and Dynamics*, Vol. 21, No. 1, Jan.-Feb. 1998, pp. 109-115.

10. V. Kapila, A. G. Sparks, J.M. Buffington, and Q. Yan, "Spacecraft Formation Flying: Dynamics and Control," *Journal of Guidance, Control, and Dynamics*, Vol. 23, No. 3, May-June 2000, pp. 561-563.

11. A. Sparks, *Satellite Formationkeeping Control in the Presence of Gravity Perturbations*. American Control Conference, Chicago, IL, June 28-30, 2000. Vol. 2 (A01-12740 01-63), Piscataway, NJ.

12. R.K. Yedevalli and A.G. Sparks, *Satellite Formation Flying Control Design Based on Hybrid Control System Stability Analysis*. American Control Conference, Chicago, IL, June 28-30, 2000, Proceedings. Vol. 3 (A01-12793 01-63), Piscataway, NJ.

13. D.J. Irvin Jr. and D.R. Jacques, "Linear vs. Nonlinear Control Techniques for The Reconfiguration of Satellite Formations," *AIAA Guidance, Navigation, and Control Conference and Exhibit*, Montreal, Canada, Aug. 6-9, 2001. AIAA Paper 2001-4089.

14. D.T. Stansbery and J.R. Cloutier, "Nonlinear Control of Satellite Formation Flight," *AIAA Guidance, Navigation, and Control Conference and Exhibit*, Denver, CO, Aug. 14-17, 2000. AIAA Paper 2000-4436.

15. S.R. Vadali, S.S. Vaddi, K. Naik, and K.T. Alfriend, "Control of Satellite Formations," *AIAA Guidance, Navigation, and Control Conference and Exhibit*, Montreal, Canada, Aug. 6-9, 2001. AIAA Paper 2001-4028.

16. S.R. Starin, R.K. Yedavalli, and A.G. Sparks, "Spacecraft Formation Flying Maneuvers Using Linear Quadratic Regulation with No Radial Axis Inputs," *AIAA Guidance, Navigation, and Control Conference and Exhibit*, Montreal, Canada, Aug. 6-9, 2001. AIAA Paper 2001-4029.

17. C. Sabol, R. Burns, and C.A. McLaughlin, "Satellite Formation Flying Design and Evolution," *Journal of Spacecraft and Rockets* (0022-4650), vol. 38, no. 2, Apr. 2001, p. 270-278.

18. C.C. Chao, J.E. Pollard, and S.W. Janson, "Dynamics and Control of Cluster Orbits for Distributed Space Missions," Proceedings of the AAS/AIAA Space Flight Mechanics Meeting, Breckenridge, CO, Feb. 7-10, 1999. AAS Paper 99-126.

19. H. Schaub and K.T. Alfriend, "Impulsive Spacecraft Formation Flying Control to Establish Specific Mean Orbit Elements," *Journal of Guidance, Control, and Dynamics*, Vol. 24, No. 4, July-Aug. 2001, pp. 739-745.

20. Z. Tan, P. M. Bainum, and A. Strong, "The Implementation of Maintaining Constant Distance Between Satellites in Elliptic Orbits," *Advances in the Astronautical Sciences*, Vol. 105, 2000, pp. 667-683.

21. Z. Wang, F. Khorrami, and W. Grossman, *Robust Adaptive Control of Satellite Formationkeeping for a Pair of Satellites*, American Control Conference, Chicago, IL, June 28-30, 2000. Vol. 2 (A01-12740 01-63), Piscataway, NJ

22. M.S. de Queiroz, V. Kapila, and Q. Yan, "Adaptive Nonlinear Control of Multiple S/C Formation Flying," *Journal of Guidance, Control, and Dynamics*, Vol. 23, No. 3, May-June 2000, p. 385-390.

23. Q. Yan, G. Yang, V. Kapila, and M.S. de Queiroz, "Nonlinear Dynamics and Output Feedback Control of Multiple Spacecraft in Elliptic Orbit," Proceedings of the American Control Conference, Chicago, IL, June 28-30, 2000, Vol. 2, Piscataway, NJ.

24. P. Gurfil and N. J. Kasdin, "Dynamics and Control of Spacecraft Formation Flying in Three-Body Trajectories," *AIAA Guidance, Navigation, and Control Conference and Exhibit*, Montreal, Canada, Aug. 6-9, 2001. AIAA Paper 2001-4026.

25. D.J. Scheeres and N.X. Vinh, "Dynamics and control of relative motion in an unstable orbit," *AIAA/AAS Astrodynamics Specialist Conference*, Denver, CO, Aug. 14-17, 2000. AIAA Paper 2000-4135.

26. B.T. Barden and K.C. Howell, "Fundamental Motions Near Collinear Libration Points and Their Transitions," *The Journal of the Astronautical Sciences*, Vol.46, No. 4, 1998, pp.361-378.

27. B.T. Barden and K.C. Howell, "Formation Flying in the Vicinity of Libration Point Orbits," *Advances in Astronautical Sciences*, Vol. 99, Pt. 2, 1998, pp. 969-988.

28. K.C. Howell and B.T. Barden, "Trajectory Design and Stationkeeping for Multiple Spacecraft in Formation Near the Sun-Earth L_1 Point," *IAF, International Astronautical Congress*, 50th, Amsterdam, Netherlands, Oct. 4-8, 1999. IAF/IAA Paper 99-A707.

29. N.H. Hamilton, *Formation Flying Satellite Control Around the L_2 Sun-Earth Libration Point*, M.S. Thesis, George Washington University, Washington, DC, December 2001.

30. D. Folta, J.R. Carpenter, and C. Wagner, "Formation Flying with Decentralized Control in Libration Point Orbits," International Symposium: Spaceflight Dynamics, Biarritz, France, June, 2000.

31. K.C. Howell and J.P. Anderson, "Generator User's Guide", Version 3.0.2, IOM AAE-0140-012, July 2001.

32. A.E. Bryson and Y. Ho, *Applied Optimal Control : Optimization, Estimation, and Control*, New York: Hemisphere Pub. Corp., 1975.

33. K.C. Howell and H.J. Pernicka, "Numerical determination of Lissajous trajectories in the restricted three- body problem." *Celestial Mechanics* , Vol. 41, No. 1-4, 1987/88, p. 107- 124.

34. K.C. Howell and J.J. Guzman, "Generator", IOM AAE-0140-010, 2001.

35. G. Chen, J. Fang, Y. Hong, and H. Qin, *Introduction to Chaos Control and Anti-Control*, Advanced Topics in Nonlinear Control Systems, World Scientific Series on Nonlinear Science. Series A, Vol. 40. pp. 193-245. World Scientific Publishing: New Jersey, 2001. Edited by T.P. Leung and H.S. Qin.

36. J.E. Slotine and W. Li, *Applied Nonlinear Control*, New Jersey: Prentice Hall, 1991.

37. NSTAR – DS-1 Technology Validation Report, http://nmp-techval-reports.jpl.nasa.gov.

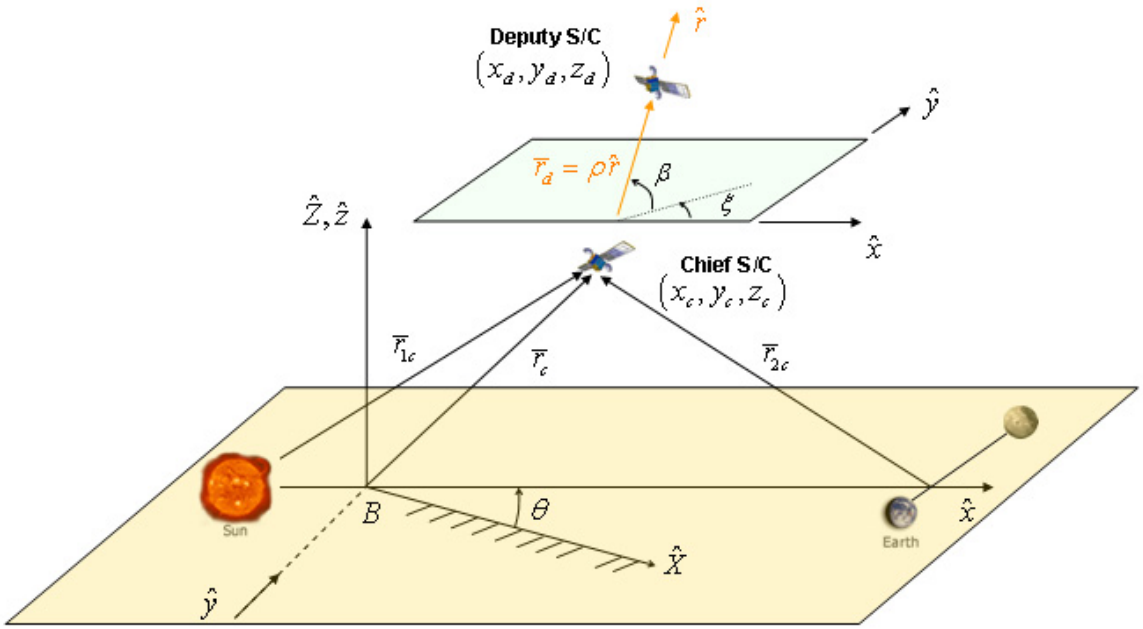

Figure 1 – Two S/C Formation Model in the Sun-Earth-Moon CR3BP

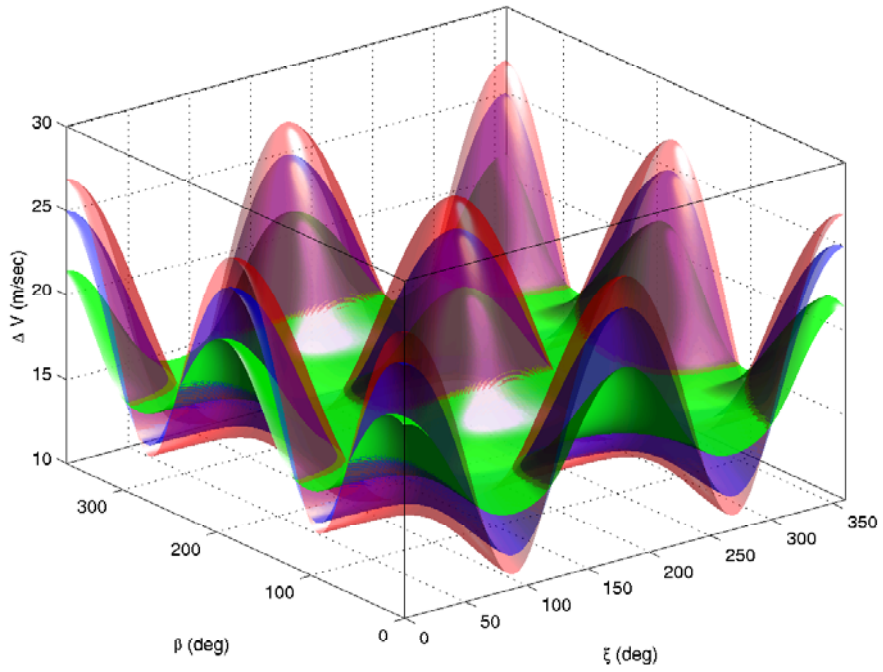

Figure 2 – Nominal Formation Keeping Cost Associated with Various 5000 km Formations, Fixed Relative to the Rotating Frame (Over 6 Months). Each Surface is Associated with a Particular L_1 Halo Orbit (A_z = 2×10^5, 7×10^5, and 1.2×10^6 km).

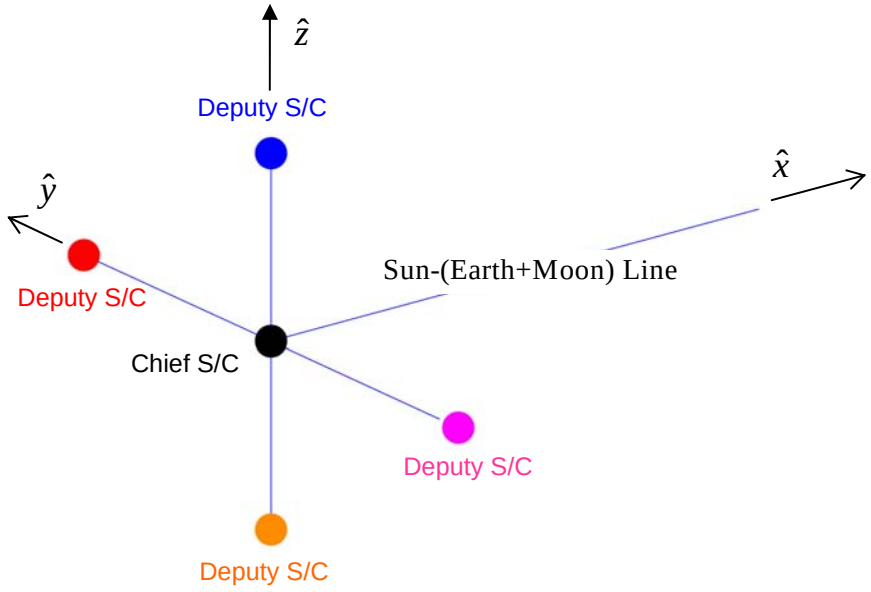

Figure 3 – Minimum Cost Formations in the Rotating Frame

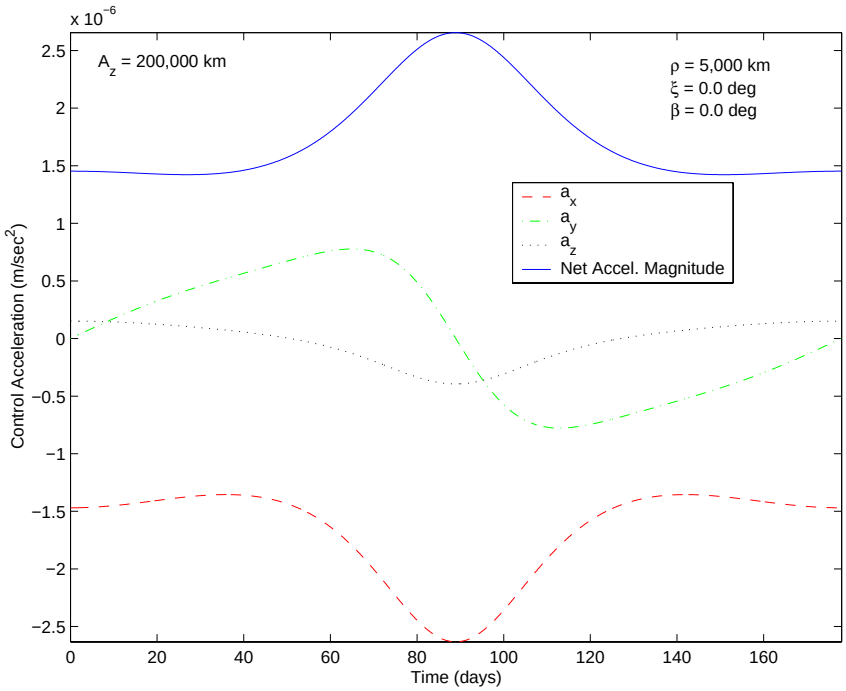

Figure 4 – Nominal Control Acceleration Required to Maintain a 5000 km Formation Fixed Relative to the Rotating Frame (Over 6 Months). Chief S/C Evolves Along a 200,000 km Halo Orbit Near the SEM L_1 Point.

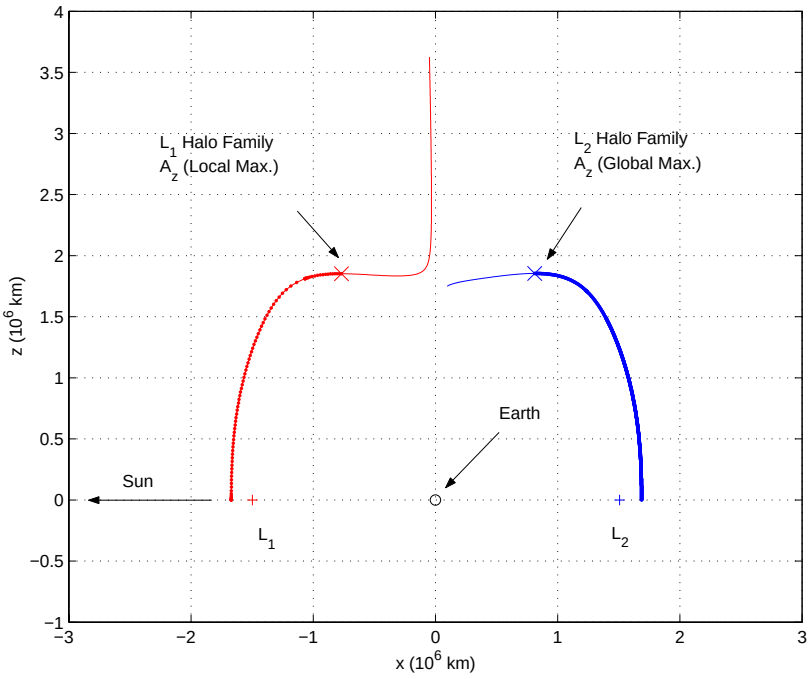

Figure 5 – L_1 and L_2 Halo Family Hodographs for the SEM System

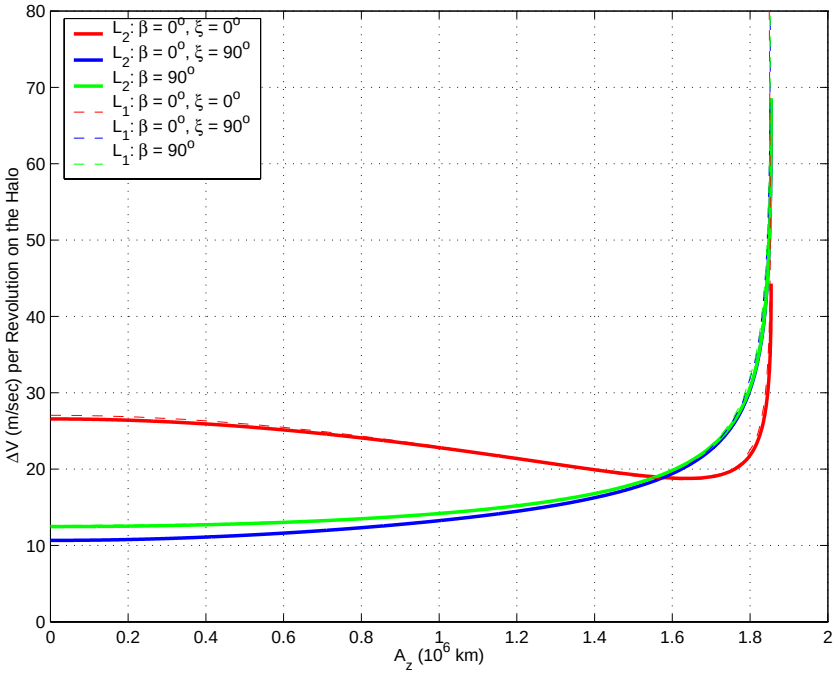

Figure 6 –Variation in Nominal Formation Keeping Cost Along the SEM L_1 and L_2 Halo Families for a 5000 km Formation Fixed Relative to the Rotating Frame (Over 6 Months)

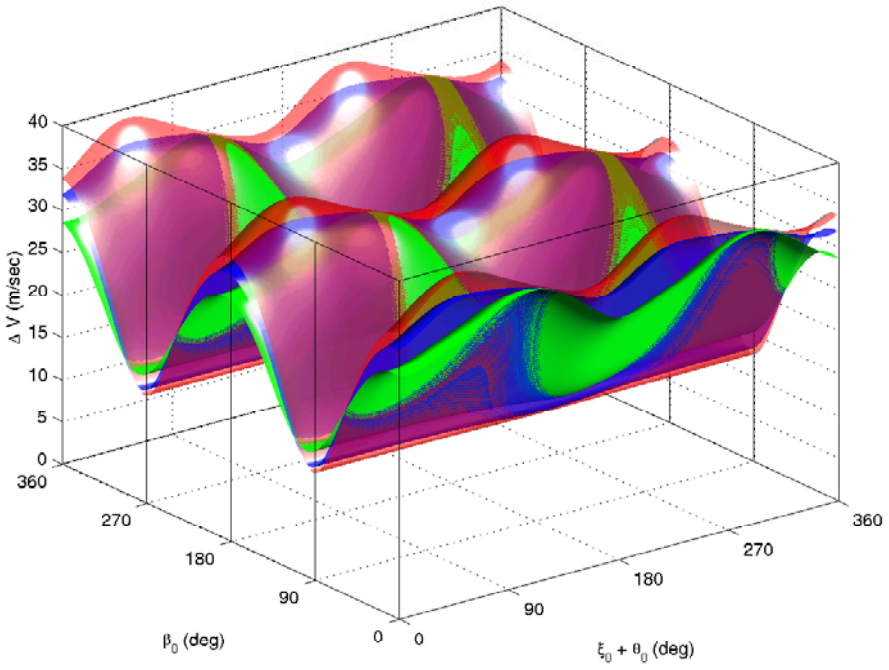

Figure 7 – Nominal Formation Keeping Cost Associated with Various 5000 km Formations, Fixed Relative to the Inertial Frame (Over 6 Months). Each Surface is Associated with a Particular L_1 Halo Orbit (A_z = 2×10^5, 7×10^5, and 1.2×10^6 km).

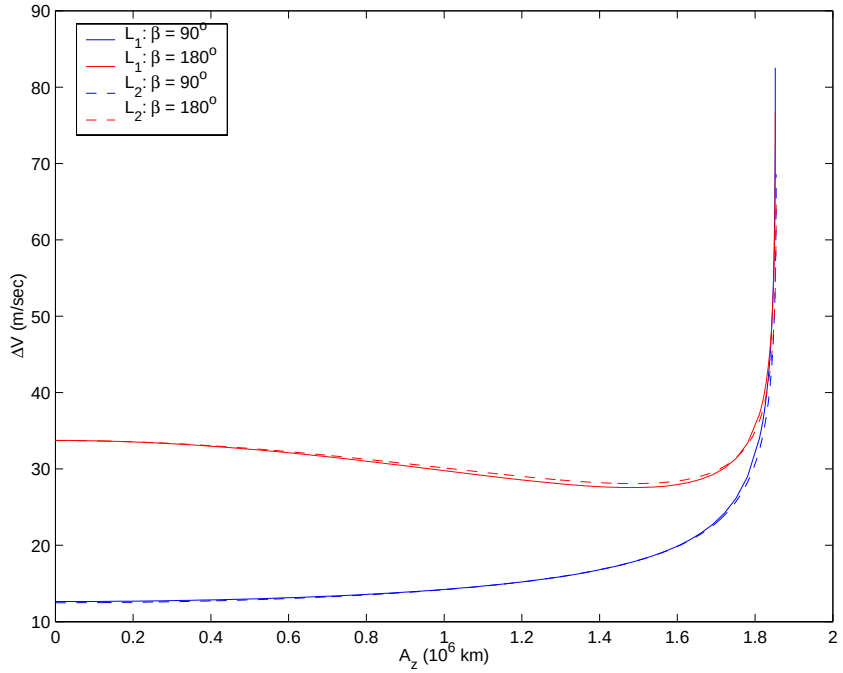

Figure 8 – Variation in Nominal Formation Keeping Cost Along the SEM L_1 and L_2 Halo Families for a 5000 km Formation Fixed Relative to the Inertial Frame (Over 6 Months)

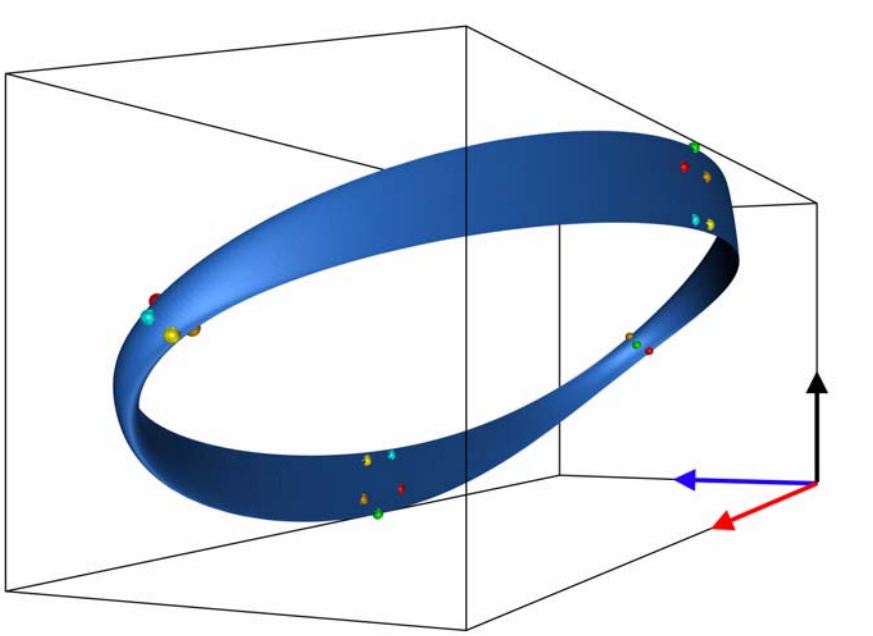

Figure 9 – Torus Near a 200,000 km Halo Orbit near the SEM L_1 Point

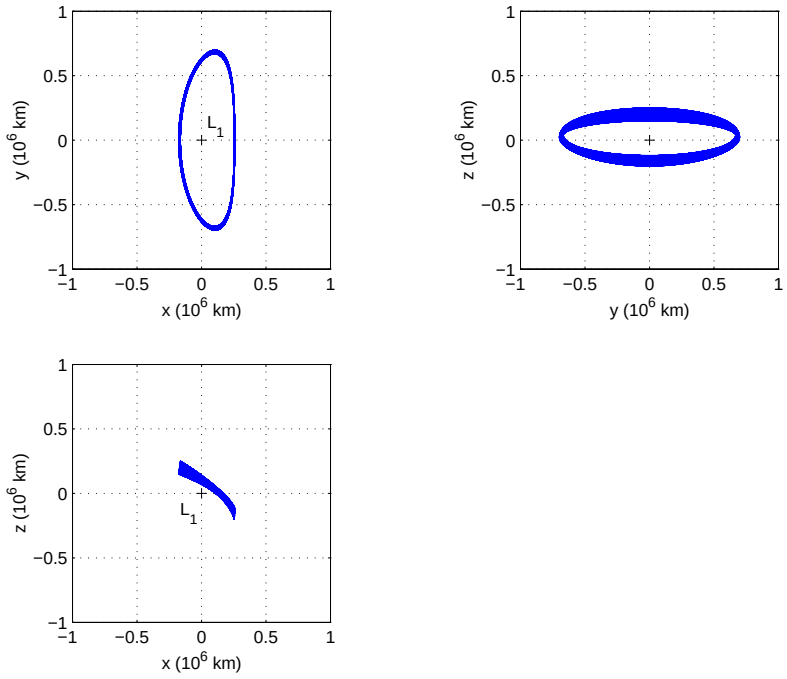

Figure 10 – Quasi-Periodic Toroidal Deputy Path Around a 200,000 km SEM L_1 Halo Orbit

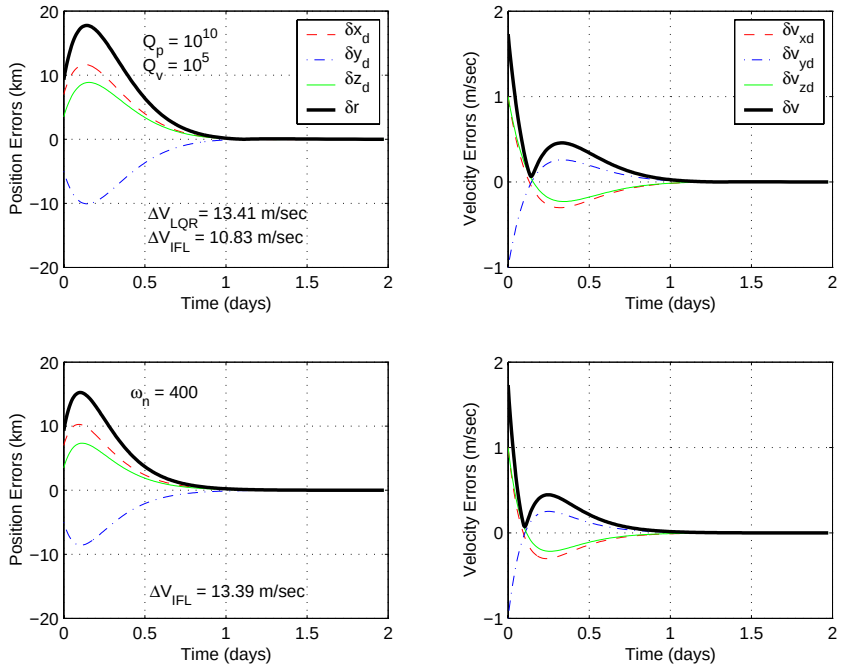

Figure 11 – LQR ($Q_p=10^{10}$, $Q_v=10^5$) vs. IFL (ω_n = 1000) Error Response for Deputy S/C in a 5000 km Formation, Fixed Relative to the Rotating Frame (Over 6 Months), Near a 200,000 km L_1 Halo Orbit

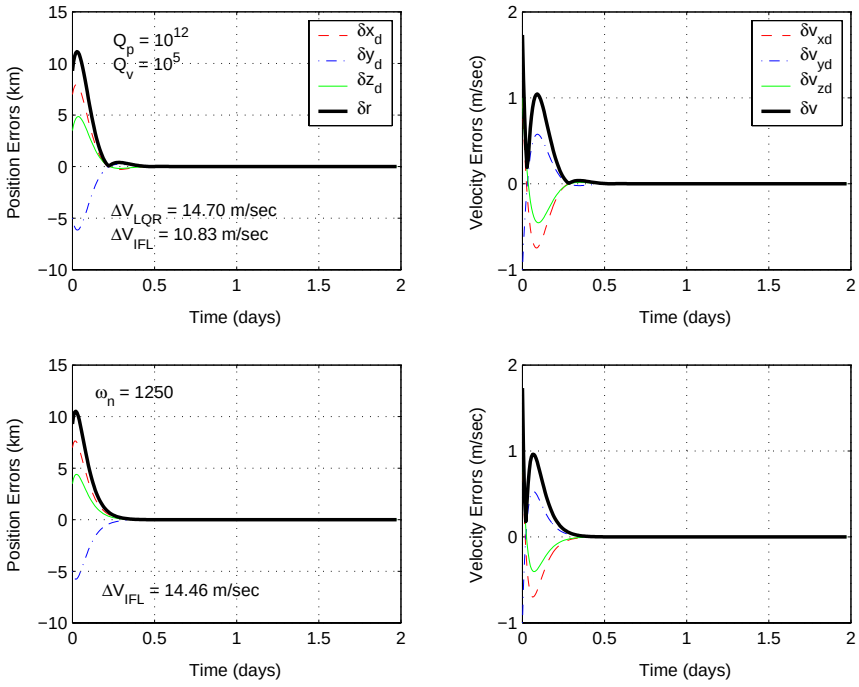

Figure 12 – LQR ($Q_p=10^{12}$, $Q_v=10^5$) vs. IFL (ω_n = 1250) Error Response for Deputy S/C in a 5000 km Formation, Fixed Relative to the Rotating Frame (Over 6 Months), Near a 200,000 km L_1 Halo Orbit

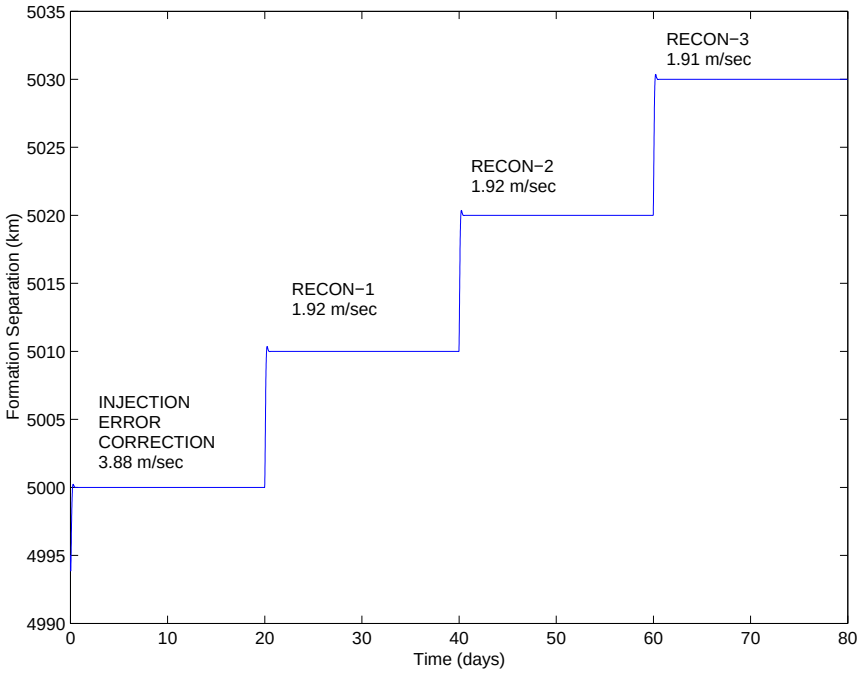

Figure 13 – LQR Applied to Formation Reconfiguration ($Q_p=10^{12}$, $Q_v=10^5$) (Correction ΔV 's Listed Do Not Include Nominal Formation Keeping Costs)

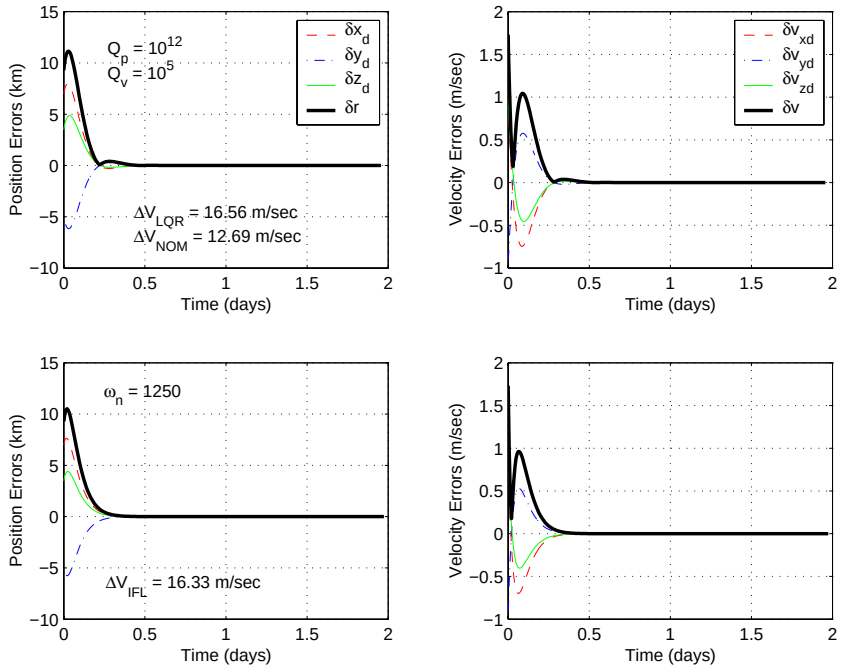

Figure 14 – LQR ($Q_p=10^{12}$, $Q_v=10^5$) vs. IFL (ω_n = 1250) Error Response for Deputy S/C in a 5000 km Formation, Fixed Relative to the Inertial Frame (Over 6 Months), Near a 200,000 km L_1 Halo Orbit

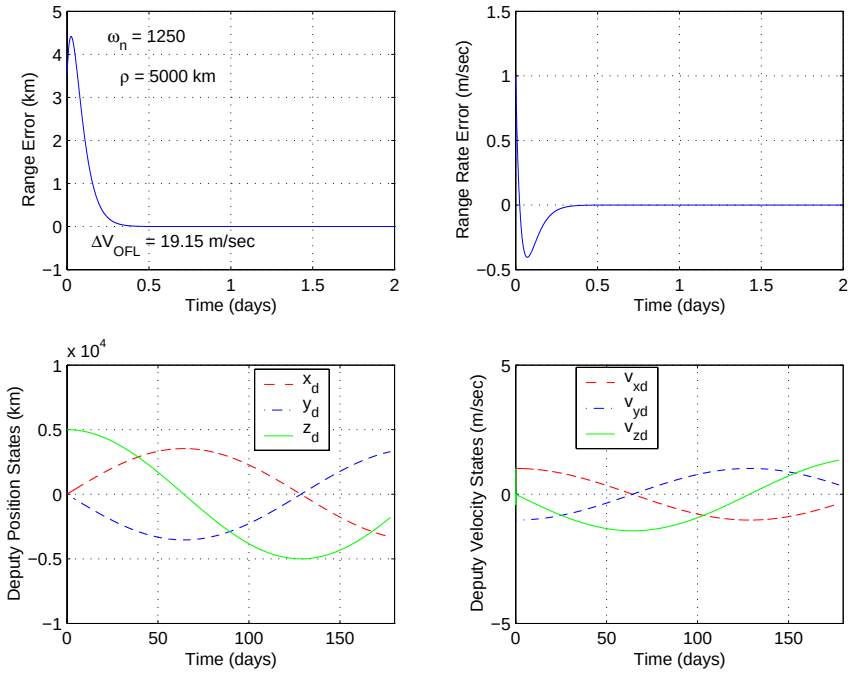

Figure 15 – OFL Controller Response to Injection Errors (ω_n = 1250) for Deputy S/C in a 5000 km Formation, with No Orientation Constraints (Over 6 Months), Near a 200,000 km L_1 Halo Orbit

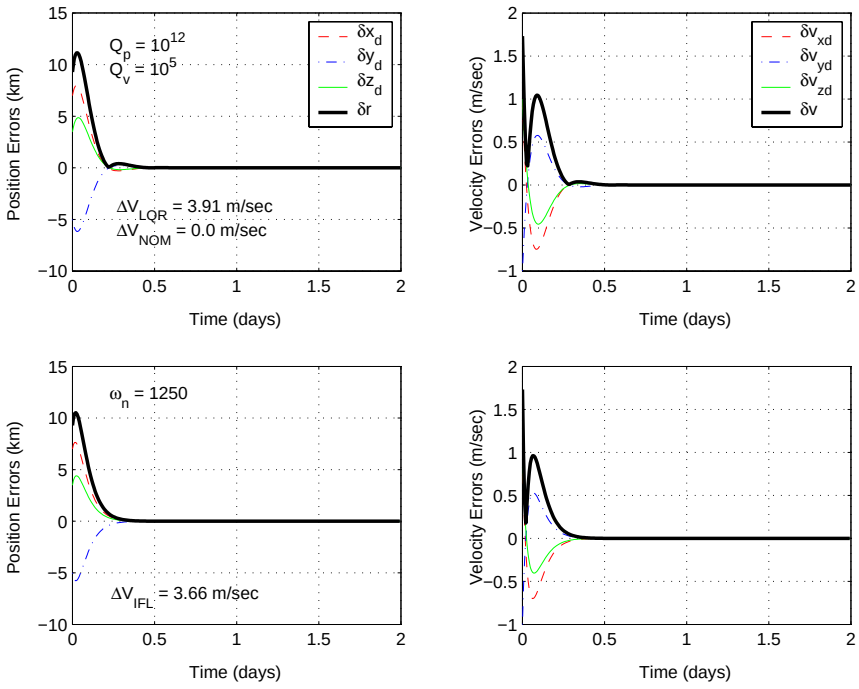

Figure 16 – LQR (Q_p=10^{12}, Q_v=10^5) vs. IFL (ω_n = 1250) Error Response for Deputy S/C Evolving Along Quasi-Periodic Orbit (Torus) in the Vicinity of a 200,000 km L_1 Halo Orbit

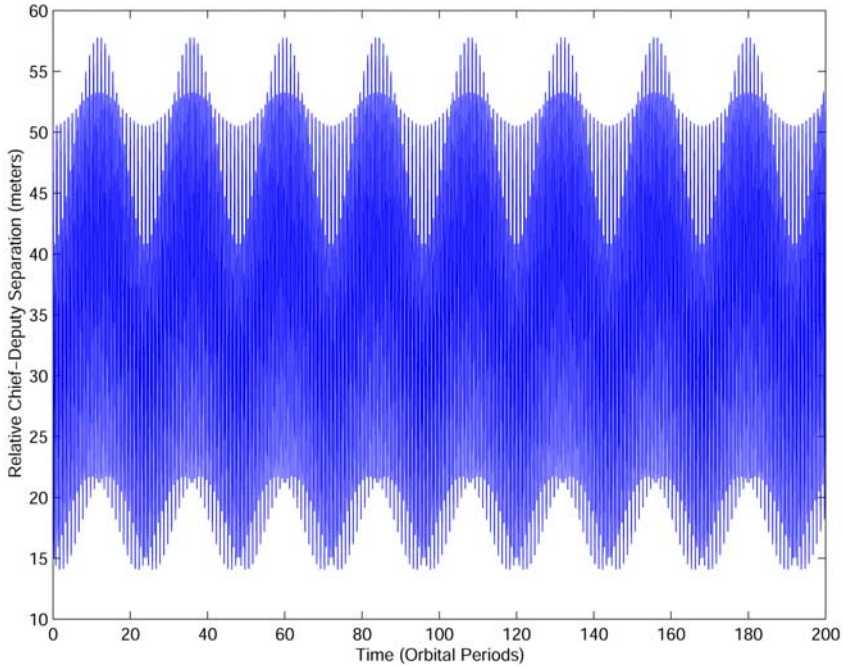

Figure 17 – Relative S/C Separation Along Quasi-Periodic Orbit (Torus) For a Small Two-Spacecraft Formation Near a 200,000 km SEM L_1 Halo Orbit

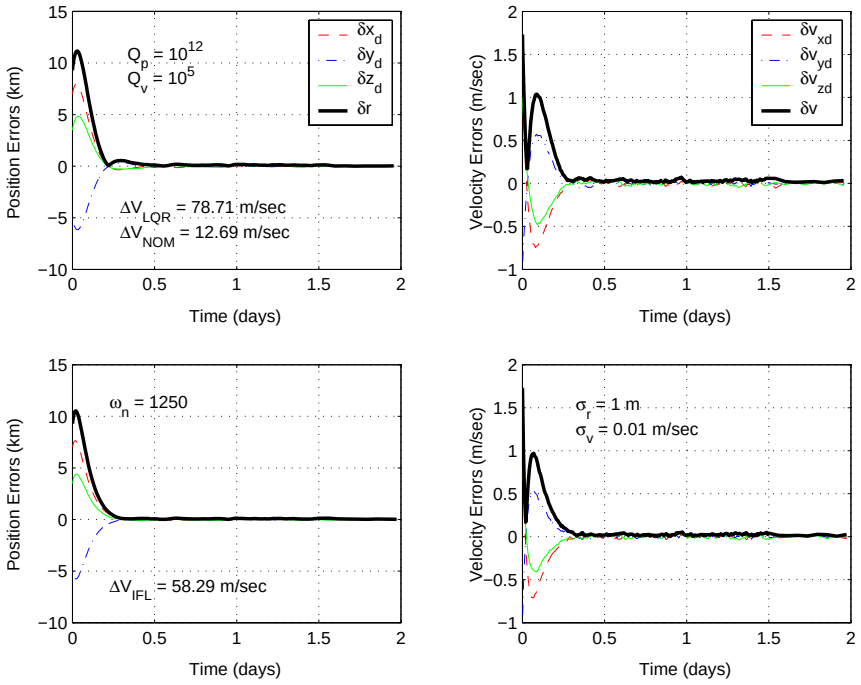

Figure 18 – LQR ($Q_p=10^{12}$, $Q_v=10^5$) vs. IFL (ω_n = 1250) Error Response for Deputy S/C in a 5000 km Formation, Fixed Relative to the Inertial Frame (Over 6 Months), Near a 200,000 km L_1 Halo Orbit. Tracking Errors on the order of 1 m and 10 mm/sec Included.

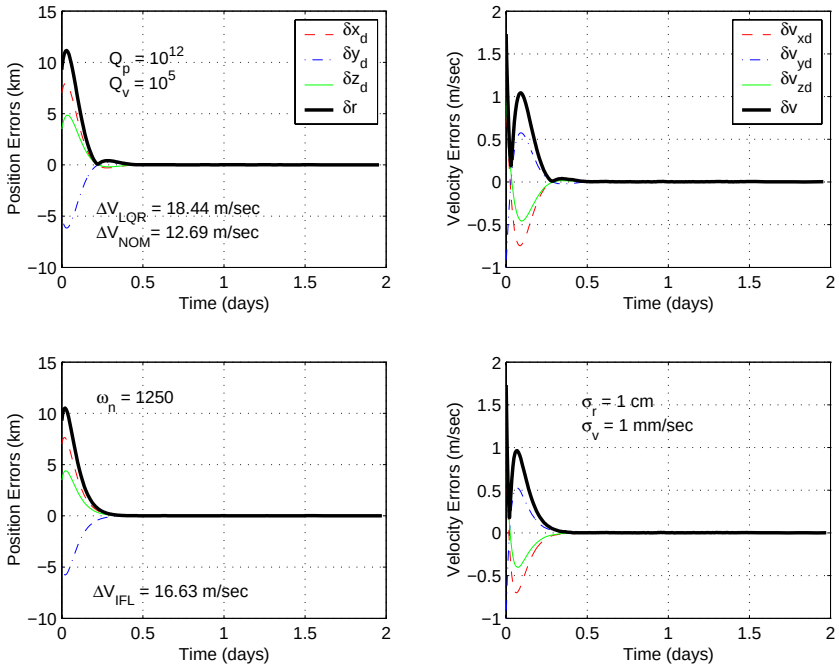

Figure 19 – LQR ($Q_p=10^{12}$, $Q_v=10^5$) vs. IFL (ω_n = 1250) Error Response for Deputy S/C in a 5000 km Formation, Fixed Relative to the Inertial Frame (Over 6 Months), Near a 200,000 km L_1 Halo Orbit. Tracking Errors on the order of 1 cm and 1 mm/sec Included.